Supporting Information

.....

pH-Responsive Covalent Organic Network: Morphology Change Leads to Capture and Removal of Phosphate Ions from Water

Gunanka Hazarika,[a] Sribash Das,[b] Niku Moni Das,[b] Debasis Manna*[ab]

[a]Centre for the Environment, Indian Institute of Technology Guwahati, Assam-781039, India
[b]Department of Chemistry, Indian Institute of Technology Guwahati
Assam-781039, India, E-mail: dmanna@iitg.ac.in.

1. General information:

All reagents were purchased from Sigma-Aldrich, Merck, Himedia and other commercial sources and used directly without further purification. The column chromatography was performed using 60–120 mesh silica gels. Reactions were monitored by thin-layer chromatography (TLC) on silica gel 60 F254 (0.25 mm). The ^{1}H NMR and ^{13}C NMR were recorded at 400 or 600 and 100 or 151 MHz with Varian AS400 spectrometer and Brucker spectrometer, respectively. The chemical shifts were reported in parts per million (δ) using DMSO-d_6, $CDCl_3$ as internal solvent. The coupling constant (J values) and chemical shifts (δ_{ppm}) were reported in Hertz (Hz) and parts per million (ppm), respectively, downfield from tetramethylsilane using residual chloroform (d = 7.24 for ^{1}H NMR, d = 77.23 for ^{13}C NMR) as an internal standard. Multiplicities are reported as follows: s (singlet), d (doublet), t (triplet), m (multiplet), and br (broadened). High-resolution mass spectra (HRMS) were recorded at Agilent Q-TOF mass spectrometer with Z-spray source using built-in software for analysis of the recorded data.

2. Synthesis and characterization of the polymers:

2.1. Synthesis of 6-(2-bromoacetyl)-2-hydroxy-1-naphthaldehyde (A) — In a stirring solution of aluminium chloride ($AlCl_3$) (930 mg, 7 mmol, 6 equiv.) in 40 mL of dichloromethane (DCM), bromoacetyl bromide (586.2 mg, 3 mmol, 2.5 equiv.) was gradually added at 0 °C. Then the temperature of the mixture was brought to 10 °C, and the mixture was stirred for 2 hours. After 2 h in that mixture, a solution of 2-hydroxynapthaldhyde (200 mg, 1.16 mmol) in DCM was added slowly, followed by raising the temperature to 45 °C, and the mixture was stirred for 24 h. Then, the reaction mixture was quenched with ice water. Next, the product was extracted with DCM. The product was purified through column chromatography using an EtOAc/Hexane 20% mixture. A yellow-coloured solid was obtained with a 78% yield.[1] **Characterization of the compound:** ^{1}H NMR (600 MHz, $CDCl_3$) δ_{ppm}: 13.36 (s, 1H), 10.85 (s, 1H), 8.48-8.48 (d, 1H), 8.47-8.45 (s, 1H), 8.22-8.20 (m, 1H), 8.14-8.12 (d, 1H), 7.28-7.28 (d, 1H), 4.56 (s, 2H).^{13}C NMR (151 MHz, $CDCl_3$) δ_{ppm}: 193.11, 190.52, 166.93, 140.17, 136.21, 131.84, 129.99, 127.93, 127.59, 126.90, 120.75, 119.42, 111.37, 77.24, 77.02, 76.81, 30.39. **HRMS (ESI) m/z:** calculated for $C_{13}H_9BrO_3$ $(M-H)^-$: 290.9662, found: 290.9962.

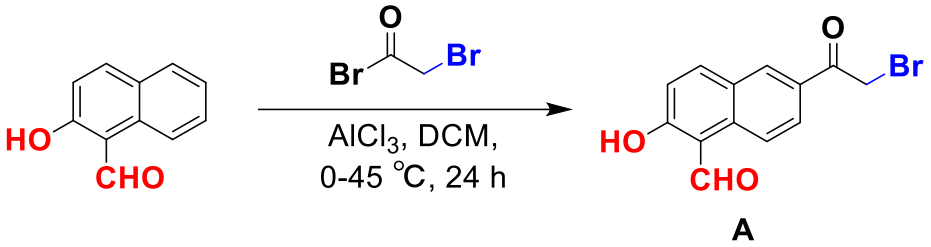

Scheme S1. Synthesis of 6-(2-bromoacetyl)-2-hydroxy-1-naphthaldehyde from 2-hydroxy-1-naphthaldehyde.

2.2. Synthesis of 6,6'-(2,2'-(((2R,3R)-2,3-dihydroxybutane-1,4 diyl)bis(sulfanediyl))bis(acetyl))bis(2-hydroxy-1-naphthaldehyde) (B) — To the stirring solution of 6-(2-bromoacetyl)-2-hydroxy-1-naphthaldehyde from 2-hydroxy-1-naphthaldehyde (500 mg, 1.7 mmol, 1.00 equiv.) in 1,4-dioxane (20 mL), 1,4-dithiothreitol (131.55 mg, 0.853 mmol, 0.5 equiv.) and trimethylamine (0.240 mL) in 1,4-dioxane was added at 0 °C. After that, the reaction mixture was stirred for 2 h at room temperature, monitored by TLC. Next, the solvent was evaporated under reduced pressure, and the product was purified through column chromatography using 30 % EtOAc / hexane, and a dark orange-coloured crystalline solid **(B)** was obtained, exhibiting a yield of 62%. **Characterization of the compound:** ^{1}H NMR (600 MHz, DMSO-d_6) δ_{ppm}: 12.21 (s, 2H), 10.78 (s, 2H), 9.02-9.01 (d, 2H), 8.61-8.60(d, 2H), 8.27-8.26 (d, 2H), 8.10-8.08 (m, 2H), 7.33-7.32 (d, 2H), 5.76 (s, 1H), 4.13-4.07 (m, 2H), 3.17 (s, 4H), 2.69-2.66 (m, 2H), 2.62-2.59 (m, 2H).^{13}C NMR (151 MHz, DMSO-d_6) δ_{ppm}: 140.01, 134.81, 131.51, 131.18, 128.15, 127.16, 123.33, 120.24, 113.13, 71.56, 55.40, 49.08, 37.86, 35.33. **HRMS (ESI) m/z:** calculated for $C_{30}H_{26}O_8S_2$ $(M + Na)^+$: 601.0961, found: 601.0968 and $(M + K)^+$: 617.0701 found 617.0701.

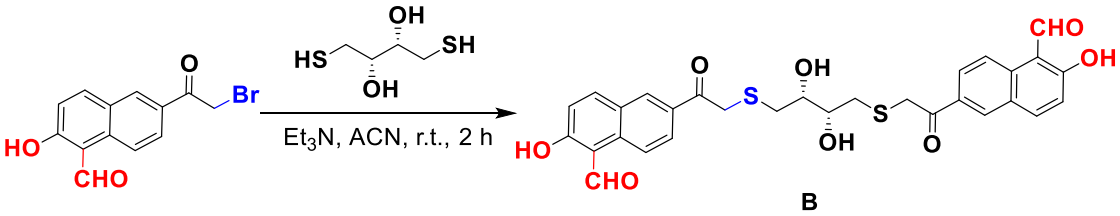

Scheme S2. Synthesis of compound 6,6'-(2,2'-(((2R,3R)-2,3-dihydroxybutane-1,4 diyl) bis(sulfanediyl)) bis(acetyl)) bis(2-hydroxy-1-naphthaldehyde).

2.3. Synthesis of tris-aminoguanidine (C) — To the stirring solution of guanidine hydrochloride (500 mg, 5.23 mmol, 1.00 equiv.) in 1,4-dioxane (30 mL), hydrazine

monohydrate (0.9 mL, 17.79 mmol, 3.40 equiv.) was added and, after that, a clear solution formed. The reaction mixture was refluxed for 3 h, and a white solid precipitate was formed. Then, the solid precipitate was filtered and washed with 1,4-dioxane (30 mL). The solid was dried under a high vacuum, affording the tris-aminoguanidine as a colourless solid with a 96% yield.[2]

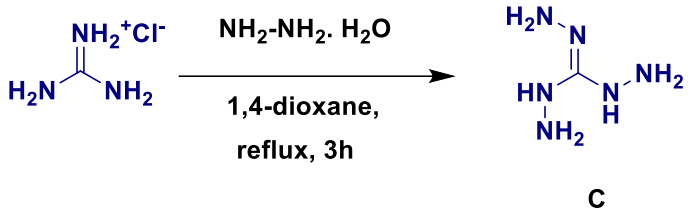

C

Scheme S3. Synthesis of tris-aminoguanidine**.**

2.4. Synthesis of ag-CON Polymer —Initially, 20 mg (0.0345 mmol) of compound 6,6'-(2,2'-(((2R,3R)-2,3-dihydroxybutane-1,4 diyl) bis(sulfanediyl)) bis(acetyl)) bis(2-hydroxy-1-naphthaldehyde) (B) and 3.29 mg (0.0228 mmol) of compound tris-aminoguanidine (C) were taken in a Pyrex tube and dissolved in a dioxane and water solution at a ratio of 1:0.3. Following this, the mixture was vacuum-sealed in the Pyrex tube and subjected to sonication for 15 minutes. Subsequently, the sealed tube was heated to 110 ˚C and left to react for a period of 3 days. A solid yellow product formed within the flask, adhering to its walls during this time. The compound was then isolated through filtration and underwent multiple washes with deionized water and various organic solvents, including ethanol, acetonitrile and tetrahydrofuran. After thorough drying in an oven at 70 ˚C for 24 hours, the resulting compound was collected for further use, exhibiting a yield of 92%. **Characterization of the compound:** solid-state FT-IR (cm^{-1}) = ~3434 cm^{-1} (s), 3317 cm^{-1} (s), 1659 cm^{-1} (s), 1615 cm^{-1} (s), 1594 cm^{-1} (s) 1291 cm^{-1} (s), and 690 cm^{-1} (s) (Figure 1A).

2.5. FT-IR spectroscopy analysis —The DTT polymer formation was analysed using FT-IR spectroscopy. The FT-IR spectra were obtained with a Bruker Optics ALPHA-E spectrometer that featured a universal Zn-Se ATR accessory. The spectra were collected within the 400-4000 cm^{-1} range.

2.6. X-ray photoelectron spectroscopy (XPS) — XPS analysis was performed to conduct the elemental analysis of the polymers. The sample was prepared utilizing the drop casting

dispersion technique. The polymer was dispersed in a water-based solution and applied onto a silicon substrate, and subsequently allowed to dry at room temperature. The analysis has identified the existence of carbon, nitrogen, and bromide ions within the polymer.

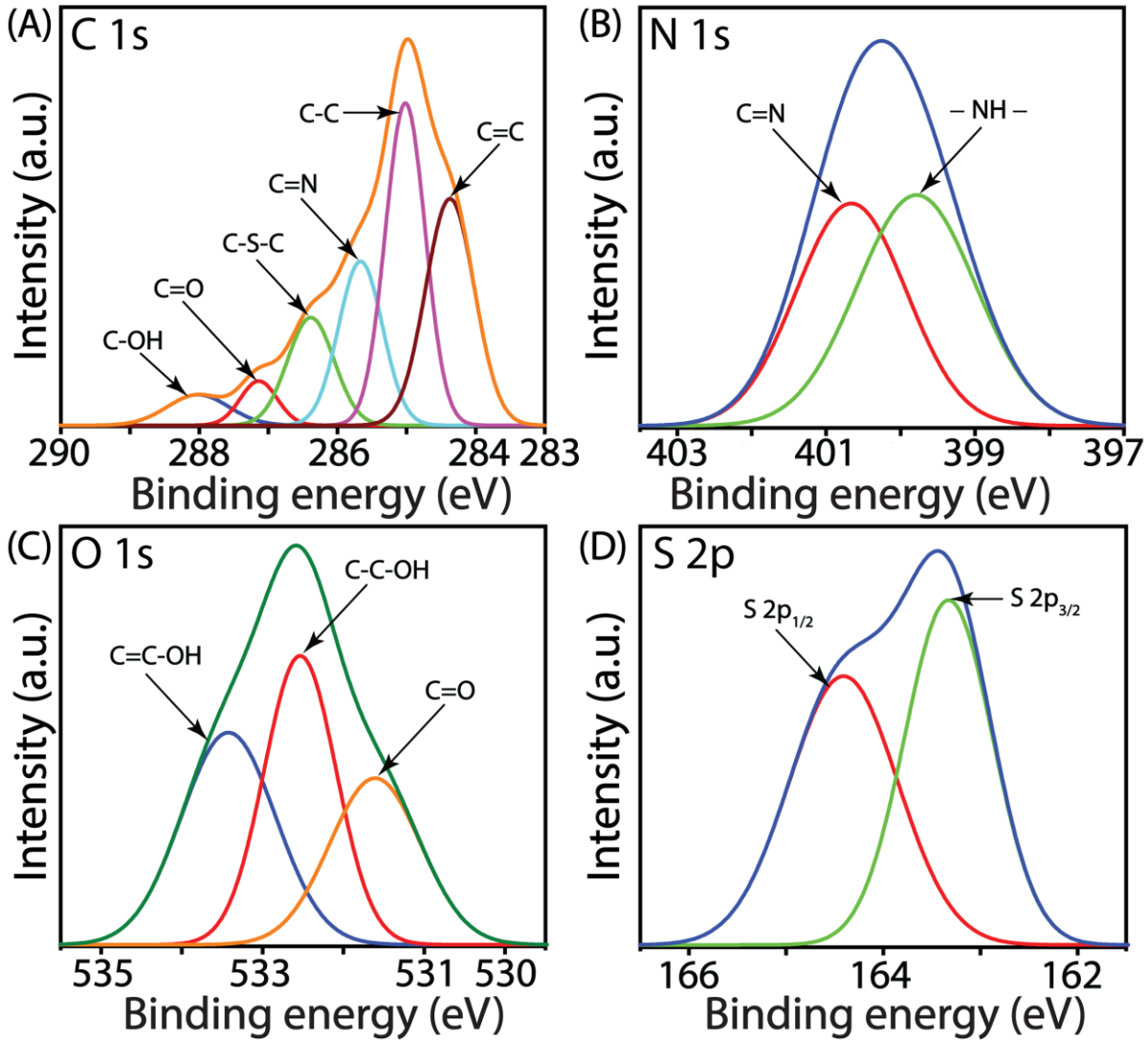

Fig. S1. XPS data profile: the deconvoluted peak of C 1s (A), N 1s (B), O 1s (C), and S 2p (D) of **ag-CON** polymer.

2.7. Powder X-ray Diffraction (PXRD) analysis — The polymer was analysed using PXRD at room temperature. The analysis was conducted using the Phillips PAN analytical diffractometer with Cu Kα radiation (α = 1.5406 Å, 40 kV, 40 mA) and the Rigaku MicroMax 007HF diffractometer.

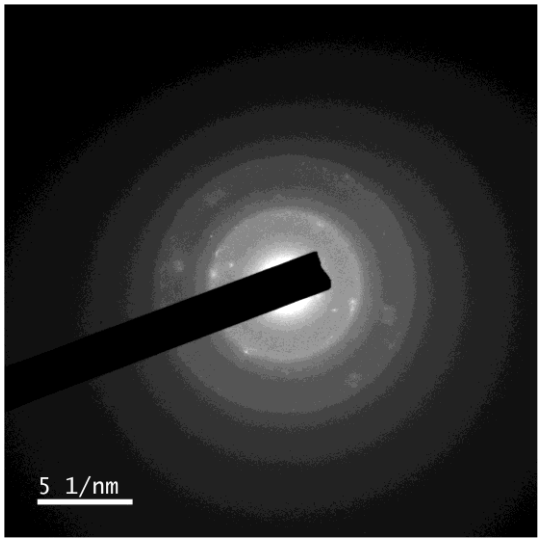

Fig. S2. Transmission electron microscopy -selected area electron diffraction (TEM-SAED) image of **ag-CON** polymer.

2.8. Scanning Electron Microscopy (SEM) — In order to conduct FESEM analysis, a minute quantity of the polymer sample (< 0.2 mg) was attached to double-sided carbon tape. The analysis was conducted using a Zeiss Sigma model OXFORD EDS FESEM instrument.

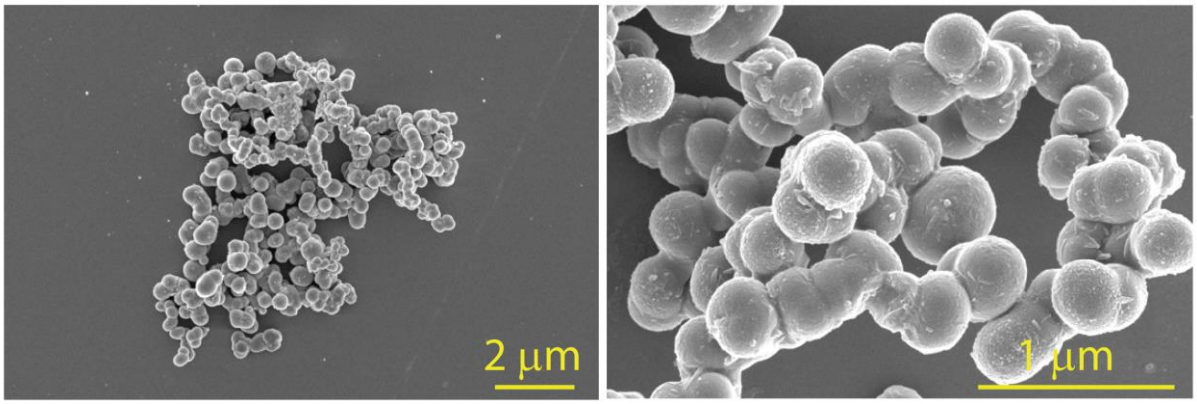

Fig. S3. Additional FESEM images of **ag-CON** polymer at different magnifications.

2.9. Transmission Electron Microscopy (TEM) — Samples were prepared for TEM analysis using the drop-cast method. At first, a small quantity of the polymer was dispersed in milli-Q water, and 10 µL of the suspension solution was deposited onto a carbon-coated copper grid and left to settle for 5 minutes. Following the gentle blotting of the grid with filter paper, it was allowed to dry overnight at room temperature. The transmission electron microscope utilized for TEM imaging was the JEOL JEM 2100, operating at a maximum accelerating voltage of 200 kV.

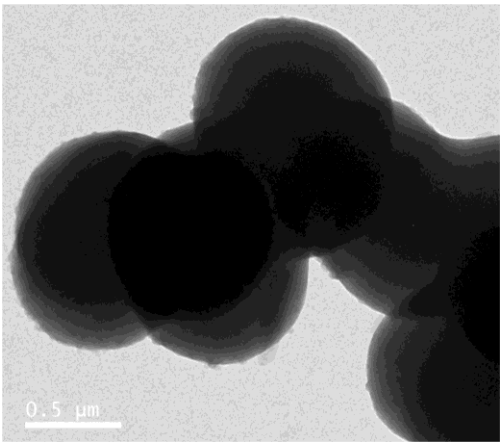

Fig. S4. Additional TEM image of **ag-CON** polymer.

2.10. Atomic Force Microscopy (AFM) — For analysis using Atomic Force Microscopy (AFM), the samples were prepared using the drop-casting technique. 5 µL of polymer suspension in milli-Q water solutions is placed on a silicon wafer and allowed to dry overnight at room temperature. AFM images were captured to analyse the morphology and height profile of the polymer. Asylum AFM AC 240 TS-R3 silicon cantilever probes were used to image the samples. Images of the samples were acquired and analysed through standard AC mode imaging, including topographic, amplitude, and phase images.

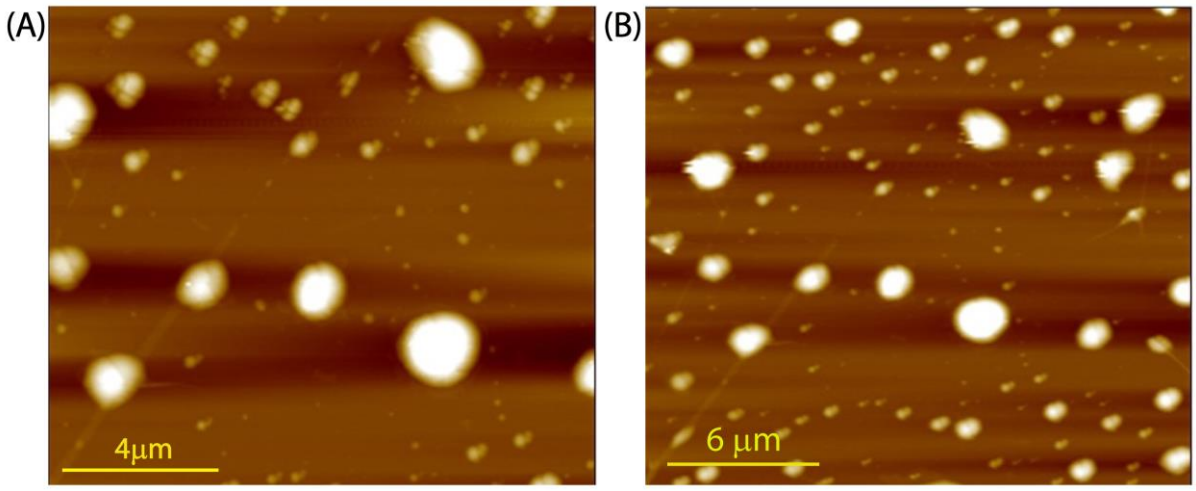

Fig. S5. Additional AFM image of **ag-CON** polymer.

2.11. FESEM-EDX and elemental mapping analysis — The polymer samples were prepared for FESEM-EDX spectroscopy and FESEM elemental analysis following the similar procedure as described earlier for FESEM.

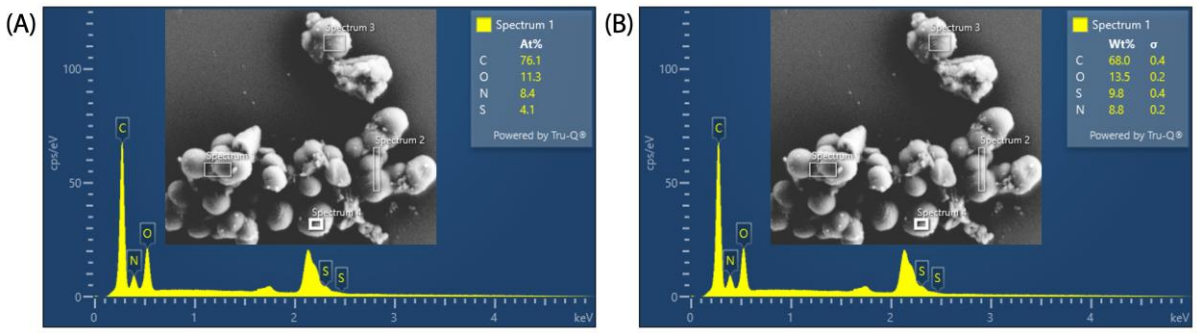

Fig. S6. FESEM-EDX analysis of **ag-CON** polymer in atomic % (A) and weight % (B).

2.12. Thermogravimetric analysis (TGA) — TGA analysis was conducted to evaluate the thermal stability of the polymer. During the experiment, a polymer sample weighing 10 mg was subjected to heating from 20 °C to 900 °C at a rate of 10 °C min^{-1} utilizing a Mettler-Toledo TG50 and SDT Q600 TG-DTA analyser under an N_2 atmosphere.

2.13. Nitrogen adsorption BET experiments — The BET adsorption experiment was conducted using Quantachrome Quadrasorb automatic and Autosorb IQ instruments. Nitrogen adsorption isotherms were measured at 77.3 K, facilitated by a liquid nitrogen bath. Prior to surface area analysis, **ag-CON** samples underwent activation at 150 °C for 24 hours under vacuum. The porosity assessment of BIP involved N_2 adsorption on activated samples at 77.3 K, while the average pore diameter was determined using Barrett–Joyner–Halenda (BJH) method. The Brunauer-Emmet-Teller (BET) surface area of BIP was calculated via multipoint BET analysis, with 'P' and 'P_0' representing the equilibrium and saturation pressure of nitrogen within the experimental setup, respectively.

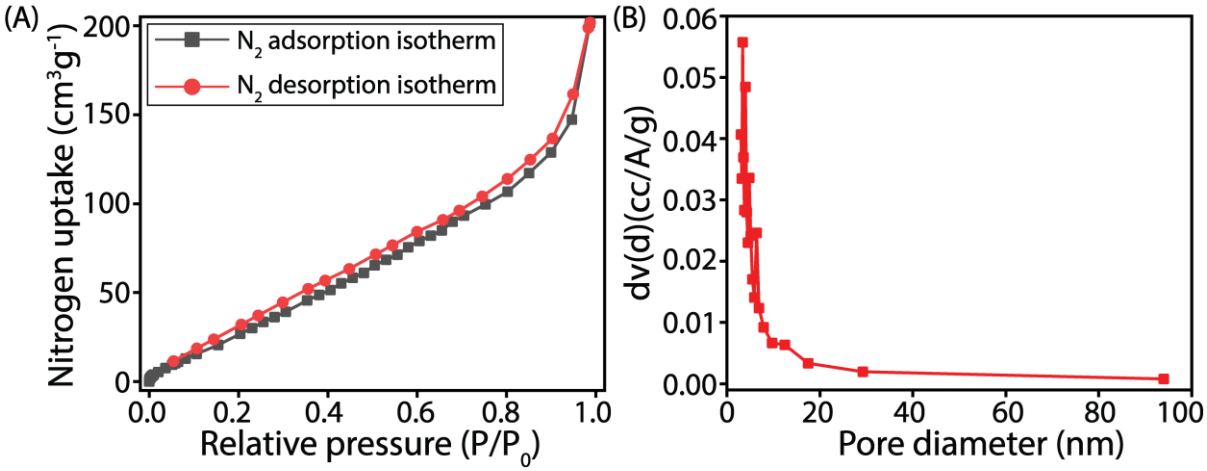

Fig. S7. Nitrogen adsorption isotherm (A) and the pore-size distribution (B) of **ag-CON** polymer.

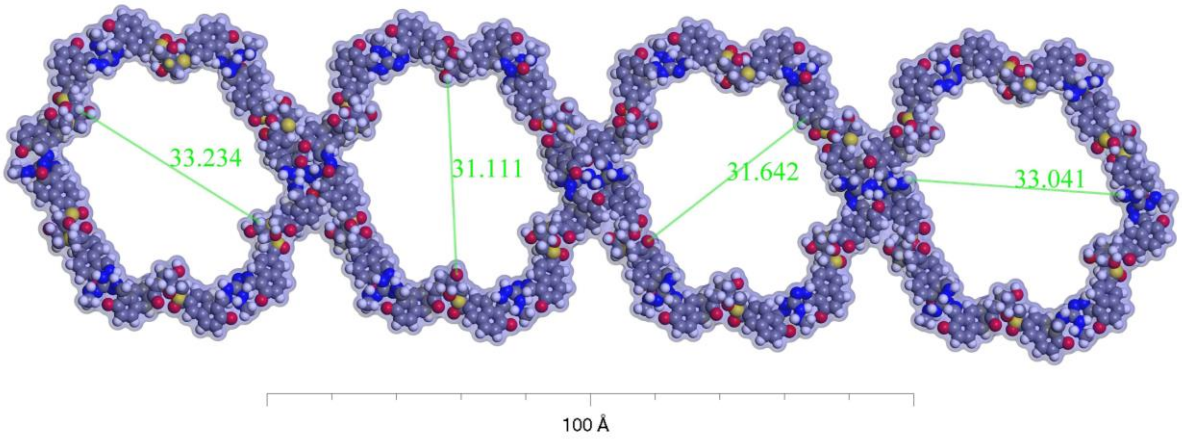

Fig. S8. Space-filling model of **ag-CON** polymer illustrating the individual pore structure, grey = carbon, red = oxygen, blue = nitrogen, yellow = sulphur, and white = hydrogen (this model was drawn in Materials Studio).

2.14. Zeta potential study— A study was conducted to determine the surface charge of the polymer at various pH levels ranging from 4 to 10 through Zeta potential analysis. The pH of the solutions was modified using 0.1 M HCl and 0.1 M NaOH. 0.5 mg of the polymer was dispersed in 2 ml of milli-Q water with varying pH levels between 4 and 10. The mixture was then agitated for 5 minutes at room temperature. Subsequently, the surface potential was measured using the Anton Paar Litesizer DLS 500 instrument at 25 °C.

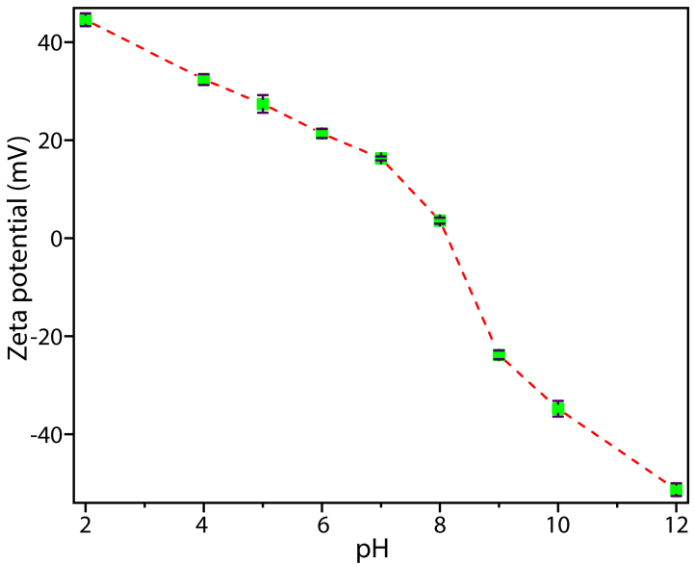

Fig. S9. Zeta potential of **ag-CON** polymer at different pH.

2.15. Tyndall effect — The dispersion of the polymer in water was confirmed using the Tyndall effect experiment. A small quantity of (≤ 5mg) **ag-CON** polymer was mixed in deionized water and sonicated for 5 min. Subsequently, the polymer solutions were illuminated with laser light with a wavelength of 640–660 nm and a maximum output of less than 1 mW, while a reference solution of pure deionized water was used as a control. This investigation elucidated the dispersion behaviour of **ag-CON** polymer in water.

2.16. DLS study of the polymer— A Dynamic Light Scattering (DLS) analysis was performed to assess the colloidal stability of the polymer in an aqueous medium. The Zetasizer Nano ZS90 instrument (Malvern, Westborough, MA) was used for the analysis. For DLS analysis, ≤ 0.5 mg of the polymers were dispersed in 1 mL of Milli-Q water and sonicated for 10 min. The hydrodynamic diameter was then measured at different time intervals (0 h, 12 h, 24 h, 36 h, and 72 h) at 25 °C. It was found that the hydrodynamic diameter remained within the range of 1000 nm during the initial 24-hour period. Consequently, all adsorption studies were performed within this timeframe following sonication.

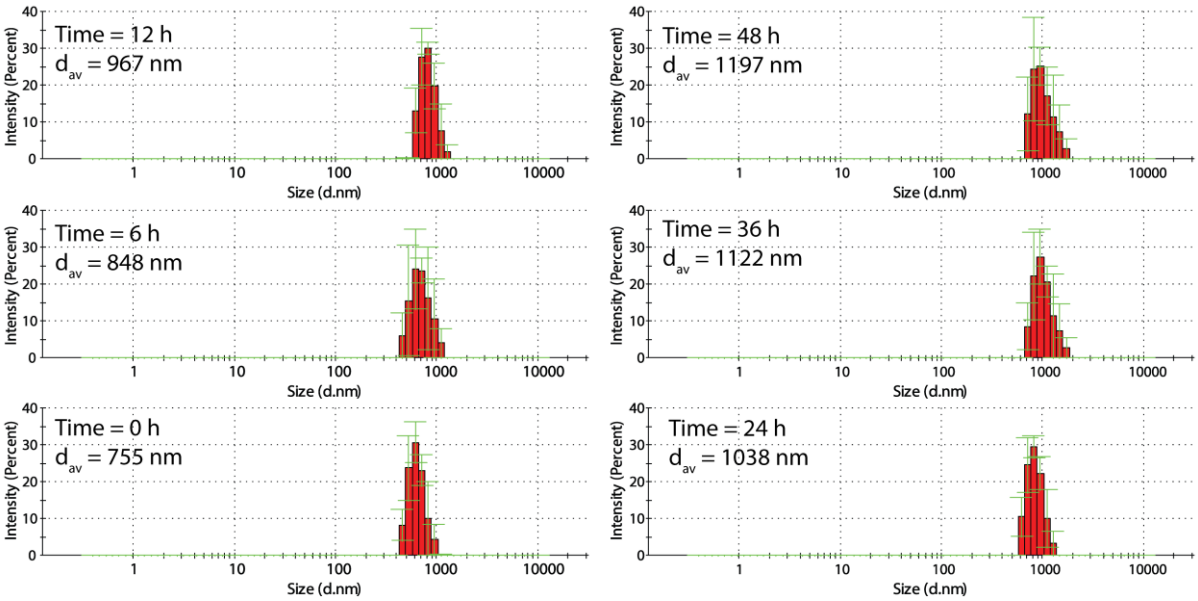

Fig. S10. DLS measurements of **ag-CON** polymer in water at different time intervals.

2.17. Chemical stability of the polymers — The polymer was subjected to treatment with various organic solvents such as acetonitrile (ACN), dichloromethane (DCM), ethyl acetate (EtOAc), methanol (MeOH), tetrahydrofuran (THF), acetone, along with 3 N hydrochloric acid (HCl) and 3 N sodium hydroxide (NaOH) solutions for a period of 14 days to evaluate its

chemical stability. Following this, their chemical stability was evaluated through Fourier Transform Infrared (FT-IR) analysis.

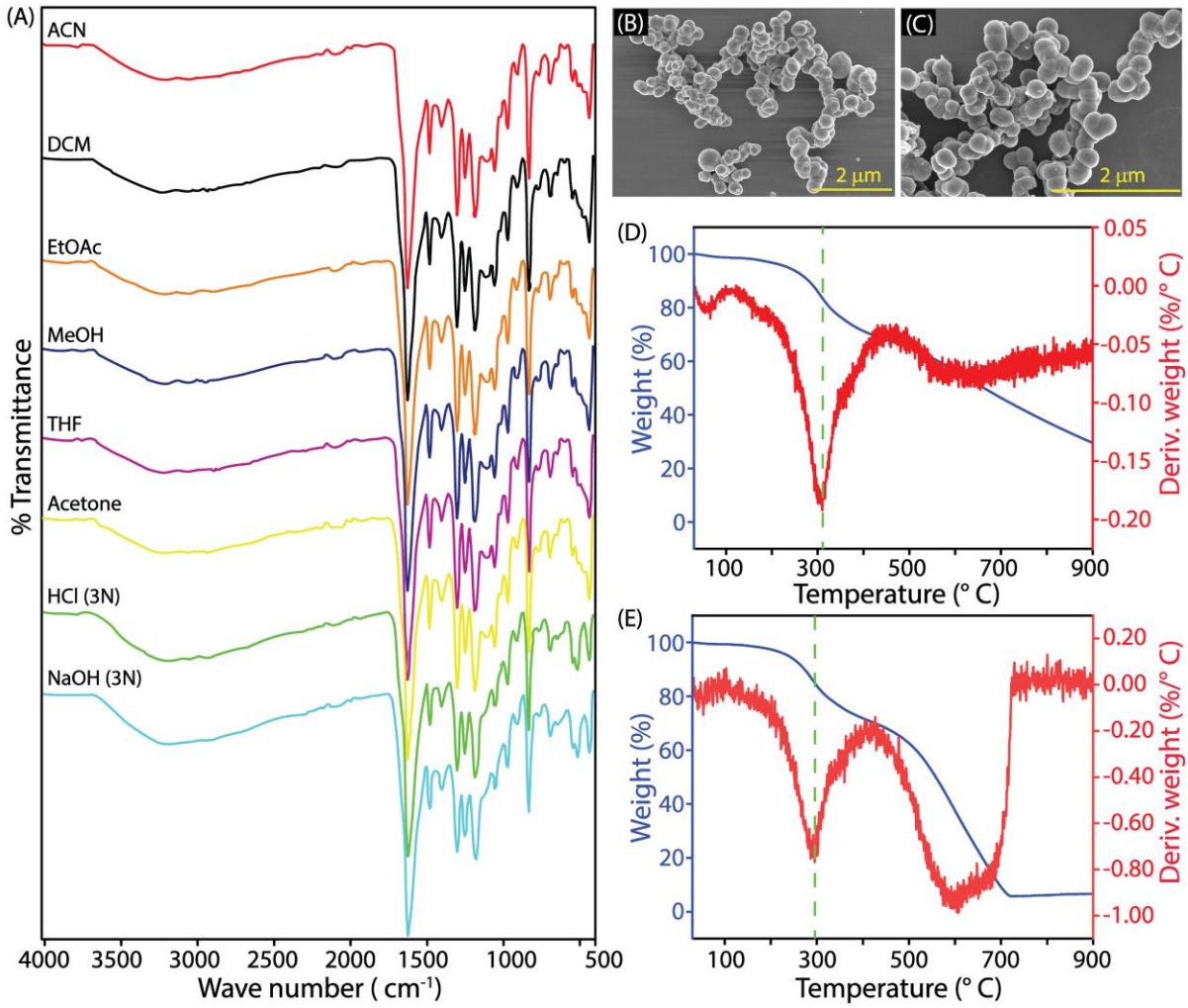

Fig. S11. FT-IR spectra of **ag-CON** polymer after the treatment (for 14 days) with ACN, DCM, EtOAc, MeOH, THF, DMF, Acetone, HCl (3 N), and NaOH (3 N) solution (A). FESEM images of **ag-CON** polymer after treatment with 3 N NaOH (A) and 3 N HCl (B) for 14 days. TGA graph of **ag-CON** polymer after treatment with 3 N NaOH (A) and 3 N HCl (B) for 14 days.

3. Selectivity experiments:

3.1. Anion Selectivity Study — To evaluate the selectivity of anions, a range of sodium salt anions (F^-, Cl^-, Br^-, NO_3^-, SO_4^{2-}, and HPO_4^{2-}) were prepared as stock solutions with a concentration of 25 ppm by dissolving them in Milli-Q water. The respective stock solution (5 mL) was mixed with 5 mg of the polymer and agitated for 6 hours. The efficacy of the polymer in adsorbing the anions was assessed using an ion chromatograph (Metrohm 792 Basic IC, Switzerland) equipped with a METROSEP A Supp 5-250/4.0 (6.1006.530) separation column (4 mm × 100 mm). Before analysis, the column was thoroughly cleansed and prepared by

running a solution containing 2 mmol of $NaHCO_3$ combined with 1.3 mmol of Na_2CO_3. The PRIMUS multi-anion solution (10 mg/kg ± 0.2% for each ionic species) from Fluka primary standard solutions was used to calibrate the instrument and column.

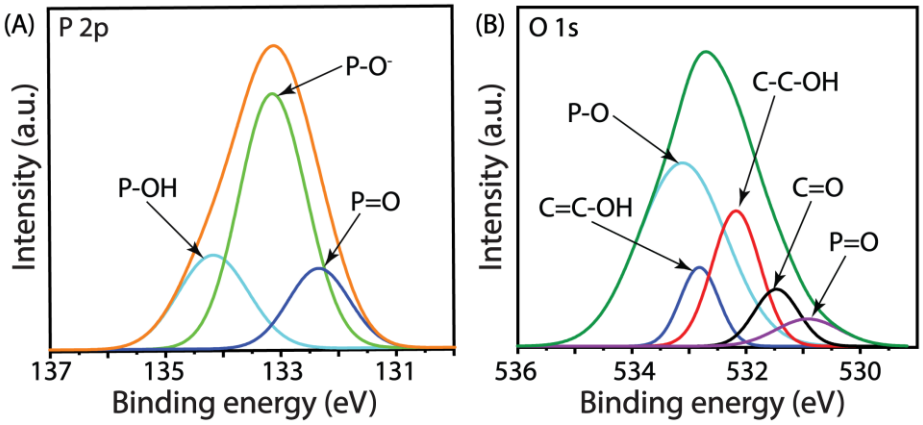

Fig. S12. XPS data profile: the deconvoluted peak of P2p (A), and O1s (B) of **ag-CON** polymer after phosphate adsorption.

3.2. Physical characterization for phosphate adsorption by ag-CON polymer — The phosphate binding ability of the **ag-CON** polymer was assessed through a series of analytical techniques, such as FTIR, XPS, FESEM-EDX, and mapping analysis. In this experiment, a 5 mg sample of the **ag-CON** polymer was subjected to treatment with a 5 mL solution containing 25 ppm of phosphate. The mixture was then sonicated for a duration of 10 minutes to ensure uniformity of the polymer. Next, the samples underwent incubation under shaking conditions for a duration of 6 hours. Following this, the samples underwent centrifugation and filtration to isolate the phosphate-adsorbed **ag-CON** polymer. Prior to the analysis, the **ag-CON** polymer with adsorbed phosphate was rinsed with milli-Q water and subjected to overnight drying using hot air.

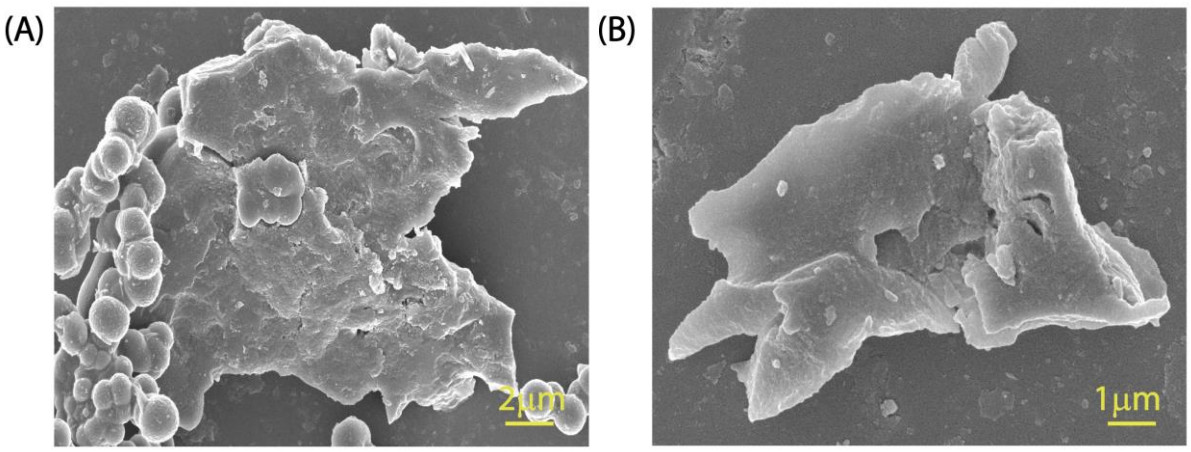

Fig. S13. FESEM images of **ag-CON** polymer after treatment with 50 ppm phosphate solution (A) and 500 ppm phosphate solution.

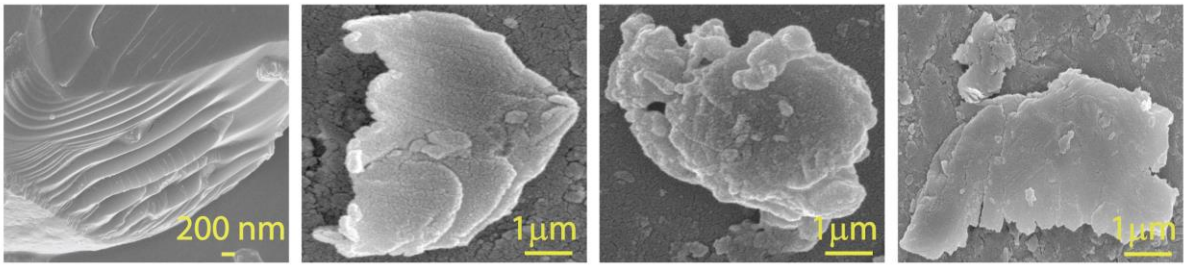

Fig. S14. Additional FESEM images of **ag-CON** polymer after the treatment with 1000 ppm phosphate solution.

4. Adsorption study:

4.1. Calculation of % ion adsorption — The following equation has been used to calculate the relative percentage of phosphate ions absorbed from water:

Percentage of adsorption (Q_{ad} %),

$$Q_{ad}(\%) = \frac{C_0 - C_e}{C_0} \times 100\% \ldots Eq.S1$$

Where, Q_{ad} is the relative percentage adsorption, C_0 and Ce are the concentrations of anions in ppm (mg/L) before and after treatment of polymers, respectively.

4.2. Calculation for adsorption capacity — The adsorption capacity of the **ag-CON** polymer was quantified using the formula denoted as Eq. (S2).

$$Q_e = \frac{(C_0 - C_e)}{m} V\ n \ldots Eq.S2$$

Where, Q_e = equilibrium adsorption capacity (mg g^{-1}), Co = initial concentration (ppm), Ce = equilibrium concentration (ppm), V = volume of solution (mL), m = amount of adsorbent (mg), and n = dilution factor.

4.3. Adsorption isotherm experiment — In order to explore the adsorption patterns, Langmuir isotherm (Equation (S3)) and Freundlich isotherm models (Equation (S4)) were used to fit the adsorption data.

$$Q_e = \frac{Q_m\ K_l\ C_e}{1\ +\ K_l\ C_e} \ldots Eq.S3$$

$$Q_e = K_f\ C_e^{1/n} \ldots Eq.S4$$

Where C_e is the equilibrium phosphate ion concentration (ppm), Q_e is the corresponding adsorption capacity (mg g^{-1}). The K_l is the Langmuir constant, and Q_m is the max adsorption capacity for the Langmuir model. The K_f and n are the Freundlich constants. For Freundlich adsorption isotherm, the K_f is associated with the adsorption capacity of the polymer. Whereas, 1/n describes the extent of adsorption (favourable 1/n < 1 or unfavourable 1/n > 2).

4.4. Adsorption kinetics equations — In order to explore the sorption mechanism, the time-dependent adsorption data were analysed by fitting using the pseudo-first-order kinetics model and the pseudo-second-order kinetics model as given in equations (S5) and (S6), respectively.

$$\ln(Q_e - Q_t) = lnQ_e - k_1 t \ldots Eq.S5$$

$$\frac{t}{Q_t} = \frac{1}{Q_e^2 k_2} + \frac{t}{Q_e} \ldots Eq.S6$$

Where Q_t and Q_e (mg g^{-1}) are the adsorption capacities of phosphate ions at time t and at equilibrium, respectively. The k_1 and k_2 (g mg sec^{-1}) are the adsorption rate constants of the pseudo-first-order equation and the pseudo-second-order equation, respectively.

5. Phosphate Adsorption Experiments:

5.1. Influence of pH on phosphate ion capture — In order to investigate the impact of pH on the adsorption of phosphate ions by the polymer, a series of adsorption experiments were conducted across a range of pH values, spanning from 4 to 10. The pH of these solutions was adjusted by utilizing 0.1 M HCl and 0.1 M NaOH. A solution containing 5 mg of the polymer and 1000 ppm of phosphate ions was prepared by mixing 5 mL of the solution at different pH levels (4, 5, 6, 7, 8, and 10). The mixture was then agitated for 6 hours at a temperature of 25 °C. Subsequently, the polymers were isolated from the solution through a process of centrifugation and filtration. The filtered supernatants were diluted 40 times in order to maintain a phosphate ion concentration in the solution that was below 25 ppm. A quantitative analysis was conducted using an ion chromatogram-based assay to determine the remaining concentration of phosphate ions in the solutions. Based on the adsorption study, it was observed that the efficiency of phosphate ion removal is highest at pH 6. However, as the acidity of the aqueous solution increases (from pH 6 to 4) or the basicity increases (from pH 8 to 12), the removal efficiency decreases. Due to the highest adsorption affinity of the polymer at pH 6, all adsorption studies were conducted exclusively at this pH.

5.2. Adsorption Isotherms — The efficiency of phosphate ion adsorption by the polymer was assessed using a Metrohm ion chromatograph (792 Basic IC, Switzerland) by passing it through a METROSEP A Supp 5-250/4.0 (6.1006.530) separation column (4 mm x 100 mm) at different concentration gradients in Mili-Q water. The analytical column was prepared by cleansing it and passing an eluent consisting of a mixture of 2 mmol $NaHCO_3$ and 1.3 mmol Na_2CO_3 before use. The instrument and column were calibrated using Fluka primary standard solutions' PRIMUS multi-anion solution (10 mg/kg ± 0.2% of each ionic species). A range of phosphate ion concentrations, from 25 to 1000 ppm, were subjected to treatment with 5 mg of polymer in 5 mL of water. The samples were then incubated under shaking conditions for a duration of 6 hours. The samples underwent centrifugation and filtration to separate the polymer that had adsorbed phosphate from the unbound phosphate ions in the supernatant. The supernatant was subsequently diluted to a concentration of 25 ppm and quantified using IC. The Langmuir and Freundlich adsorption models were employed to investigate the correlation between adsorption parameters and the equilibrium concentration of phosphate ions. At pH 6.0, the adsorption capacity of phosphate ions was determined using the Langmuir isotherm model, yielding a value of 719 mg g^{-1}.

5.3. Kinetics study — An investigation was conducted to examine the affinity of phosphate for the polymer over time by incubating 5 mg of the polymer with 1000 ppm of phosphate salt in Milli-Q water at a pH of 6. At various time intervals (20, 40, 60, 90, 120, 150, 180, 210, 240, 270, 300, 330 and 360 seconds), samples were collected, and the polymers were separated using centrifugation and filtration. The phosphate ion concentration on the filtered supernatant was measured using IC after being diluted 40 times to maintain the phosphate ion concentration below 25 ppm. The model that best fits the data is the pseudo-second-order model, which describes the adsorption rate as 0.0000663 mg g^{-1} sec^{-1}. This model is supported by the plot of t/Q_t vs. t, where Q_t represents the quantity of phosphate adsorbed at time t second. The correlation coefficient (R^2) for this model is 0.99178, indicating a strong relationship between the variables.

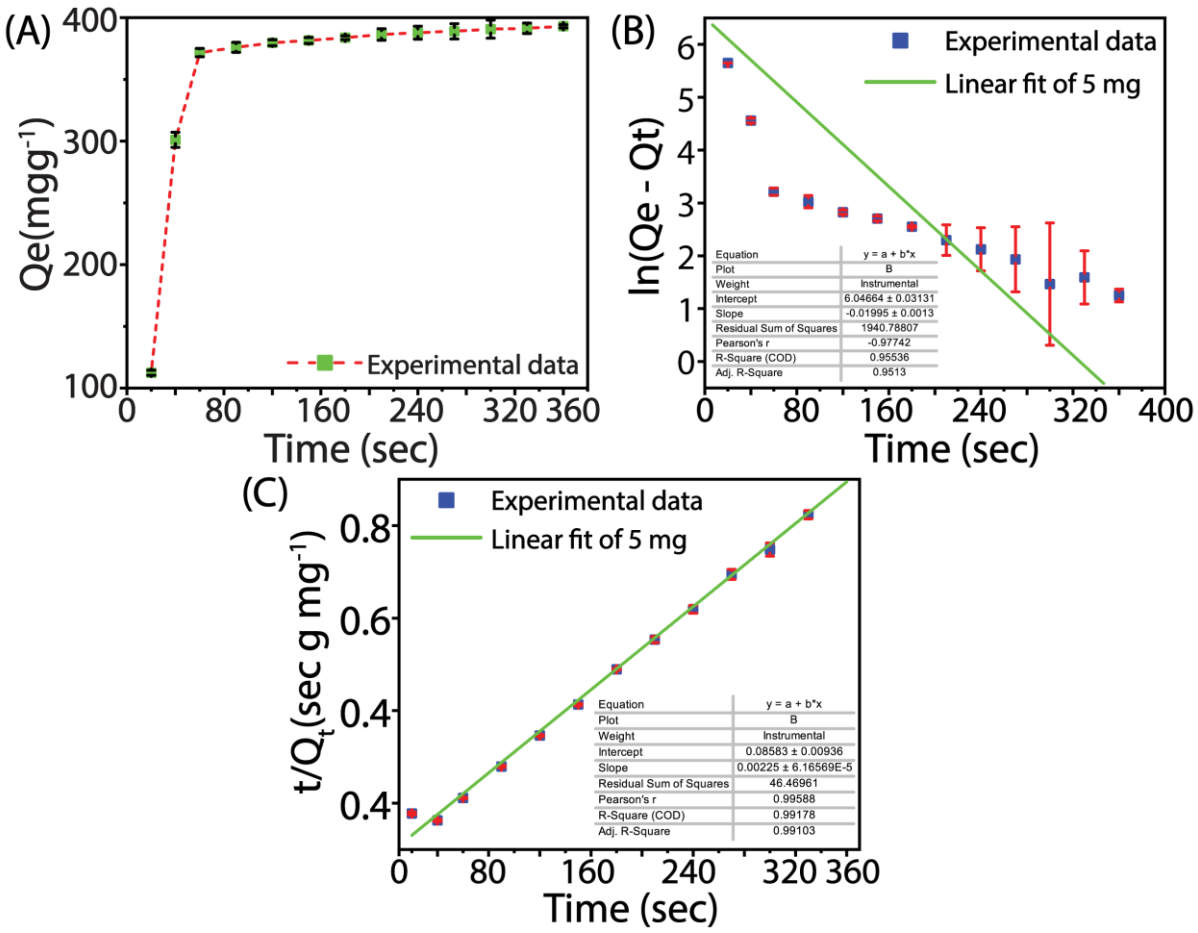

Fig. S15. Time-dependent desorption isotherm of phosphate by **ag-CON** (5 mg) at pH 6 under room temperature(A), time-dependent desorption efficiency of **ag-CON** fitted with the first order (B) and second order kinetics (C) models.

5.4. Kinetics study with different amounts of polymer — To investigate the phosphate adsorption behaviour over time, various concentrations of polymer (3 mg, 5 mg, 7 mg, and 10 mg) were combined with a 1000 ppm concentration of phosphate salt in 5 mL of Milli-Q water at pH 6. Samples were collected at various time intervals (20, 40, 60, 90, 120, 150, 180, 210, 240, 270, 300, 330 and 360 seconds), and polymers were separated using centrifugation and filtration methods. The filtered supernatant was diluted 40 times to maintain a phosphate ion concentration below 25 ppm, and then quantified using IC.

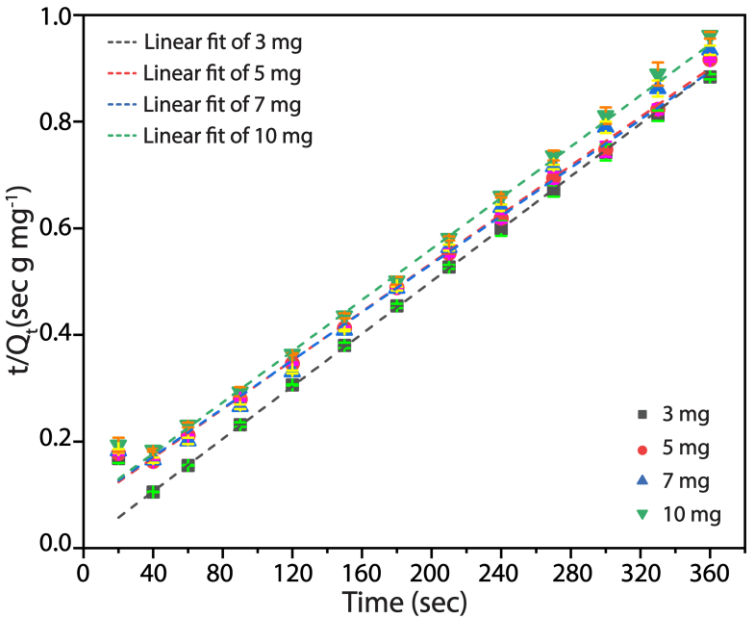

Fig. S16. Pseudo-second-order kinetics curves of phosphate adsorption on **ag-CON** (3-10 mg) at pH 6.0 under room temperature

5.5. Effect of temperature on phosphate adsorption —To investigate the influence of temperature on phosphate adsorption, four batches of 5 mL 1000 ppm phosphate solution were mixed with 5 mg of the **ag-CON** polymer and agitated individually for 6 hours at varying temperatures (298 K, 313 K, 328 K, and 343 K) at pH 6. Subsequently, the **ag-CON** polymers were separated from the phosphate solution through centrifugation, and the concentration of the phosphate solution before and after the addition of the **ag-CON** polymer was measured using IC.

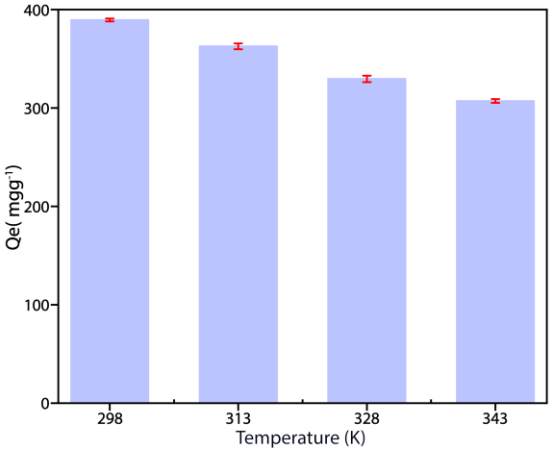

Fig. S17. The equilibrium adsorption capacity by **ag-CON** polymer at different temperatures.

5.6. Effect of counter anions on phosphate adsorption — To explore the impact of competing anions on phosphate adsorption, stock solutions of various sodium salts (F^-, Cl^-,

Br^-, NO_3^-, SO_4^{2-}, and HPO_4^{2-}) in Milli-Q water at a 1:100 concentration ratio (phosphate: other anion) were prepared. Subsequently, 5 mg of the **ag-CON** polymer was mixed with 5 mL of each salt solution and agitated for 6 hours. The efficacy of anion adsorption by the **ag-CON** polymer was assessed using IC. Remarkably, the results demonstrated that the **ag-CON** polymer displayed a pronounced preference for capturing the HPO_4^{2-} anion, even in the presence of other competing anions.

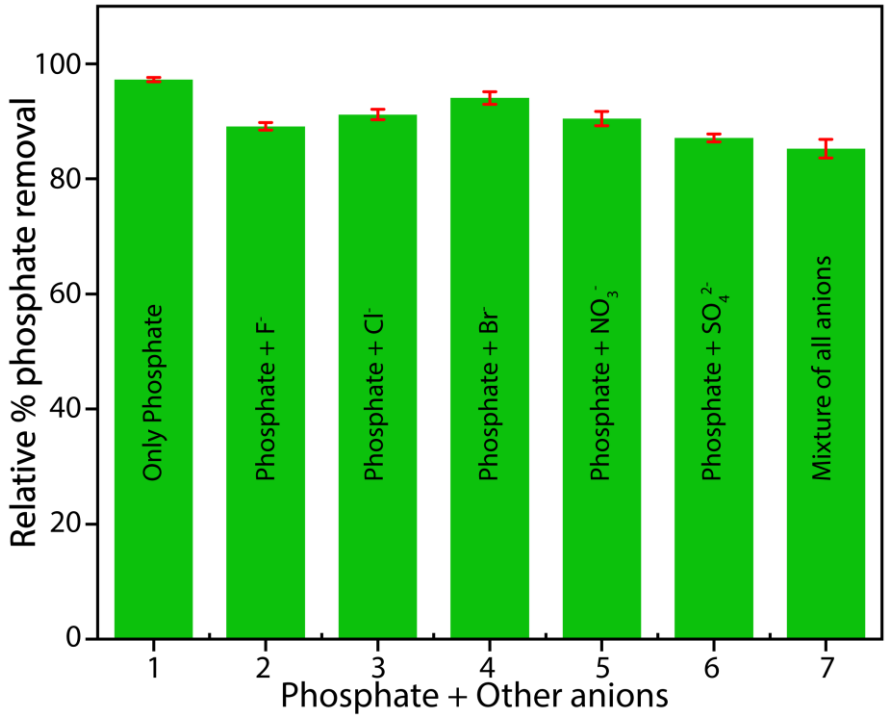

Fig. S18. Bar diagram for phosphate removal efficiency of **ag-CON** polymer in the presence of F^-, Cl^-, Br^-, NO_3^- and SO_4^{2-} anions.

5.7. Effect of counter anions on phosphate adsorption — From the effect of counter anions on phosphate ion adsorption experiments, it is clear that Cl^- ions have a negligible impact on phosphate ion adsorption by the **ag-CON** polymer. Due to the limiting solubility issue of different metal phosphates, we have selectively chosen the metal chloride salts of Na^+, K^+, Rb^+, Cs^+, Mg^{2+}, and Al^{3+} to analyse the impact of different metal ions on phosphate adsorption. To perform the experiment, stock solutions of the aforementioned metal ions along with phosphate in Milli-Q water at a 1:100 concentration ratio (phosphate: other metal ion) were prepared. Subsequently, 5 mg of the **ag-CON** polymer was mixed with 5 mL of each salt solution and agitated for 6 hours. The efficacy of the phosphate adsorption in the presence of these cations by the **ag-CON** polymer was assessed using IC. Remarkably, the results demonstrated that the **ag-CON** polymer displayed a pronounced preference for capturing the phosphate anion, even

in the presence of different metal ions. Furthermore, the results reveal that with an increased positive charge density on the metal ions, the phosphate binding affinity of the **ag-CON** polymer slightly reduces because of the affinity of metal ions binding (from monovalent to trivalent) into the coordination sites (-OH, and -NH) of the polymer.

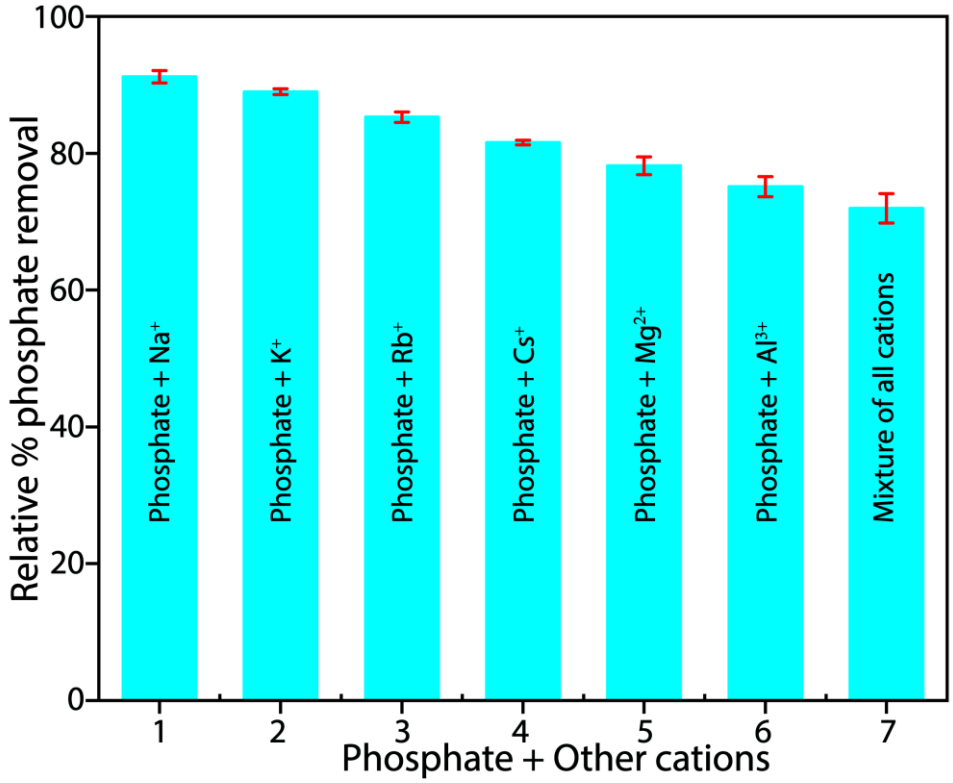

Fig. S19. Bar diagram for phosphate removal efficiency of **ag-CON** polymer in the presence of Na^+, K^+, Rb^+, Cs^+, Mg^{2+}, and Al^{3+} cations.

5.8. Low-concentration of phosphate capture study —To assess the **ag-CON** polymer's effectiveness in adsorbing low-concentration phosphate, a ~ 0.5 ppm phosphate stock solution was initially prepared. Subsequently, 5 mg of the **ag-CON** polymer was combined with 5 mL of the stock solution and agitated for 6 hours. Following this, the polymer was separated from the solution via centrifugation, and the phosphate solution's concentrations before and after treatment with the **ag-CON** polymer were measured using IC.

To evaluate the influence of interfering anions on the low-concentration phosphate adsorption process by the **ag-CON** polymer, a stock solution was prepared containing ~ 0.5 ppm phosphate ions and 100 ppm of other competing anions as mentioned above. Next, 5 mg of the **ag-CON** polymer was mixed with 5 mL of the stock solution and agitated for 6 hours. Subsequently, the **ag-CON** polymer was separated from the phosphate solution using

centrifugation, and the phosphate ion concentrations before and after treatment with the **ag-CON** polymer were quantified via IC.

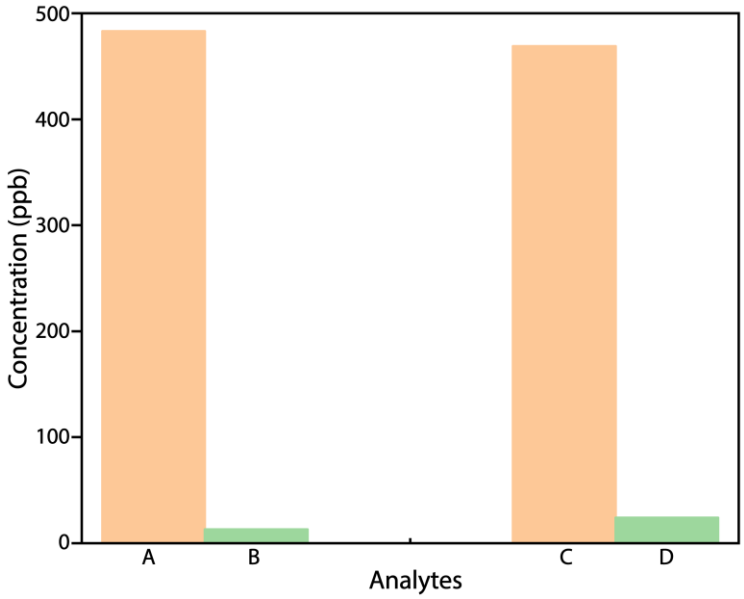

Fig. S20. Low concentration phosphate ion capture study by **ag-CON** polymer: Concentration of only phosphate ion stock solution before (A) and after (B) the treatment with **ag-CON** polymer. The concentration of phosphate ion in the phosphate and interfering anions mixture before (C) and after (D) the treatment with **ag-CON** polymer.

5.9. Phosphate removal applicability with the real phosphate contaminated wastewater— For the purpose of evaluating the efficacy of the polymer in removing phosphate from eutrophic water in real-world conditions, two wastewater samples were obtained from separate food manufacturing plants situated in Gauripur, North Guwahati, Assam, India. Table S1 displays the pH, ion concentrations, phosphate levels, and other coexisting species found in the two samples. Every sample (5 mL) was subjected to the addition of 5 mg of the polymers and underwent continuous stirring for a duration of 12 hours. Following the removal of the polymer using centrifugation and filtration, anion concentrations were analysed using ion chromatography. According to the study, the polymers effectively decreased the levels of phosphate anions to below the recommended levels set by the World Health Organization (WHO), even when other coexisting anions were present. The results presented here highlight the promising capabilities of the synthesized polymers in serving as highly efficient adsorbents for the removal of phosphate from wastewater.

Table S1. Ion chromatographic analysis demonstrating the concentrations of different competitive anions present before and after the treatment of **ag-CON** of samples A and B.

Sample	Existing anions (concentration in ppm)						pH
	F^-	Cl^-	Br^-	NO_3^-	HPO_4^{2-}	SO_4^{2-}	
Sample A	1.17 ± 0.065	12.87 ± 0.053	0.32 ± 0.037	4.10 ± 0.031	7.82 ± 0.089	11.17 ± 0.042	5.8
After **ag-CON** treatment of sample A (A′)	0.92 ± 0.027	10.55 ± 0.043	0.26 ± 0.033	3.13 ± 0.018	0.12± 0.042	7.18 ± 0.089	
Sample B	1.43 ± 0.027	12.05 ± 0.061	0.24 ± 0.032	3.61 ± 0.046	7.23± 0.068	10.35 ± 0.061	6.2
After **ag-CON** treatment of sample B (B′)	01.04 ± .041	10.12 ± .054	0.23 ± 0.026	2.56 ± 0.039	0.11 ± 0.029	6.52 ± 0.007	

5.10. Regeneration of the polymer — The reusability of the polymer was assessed through a series of batch studies involving the repetitive cycles of phosphate adsorption and desorption. During each adsorption cycle, a 5 mg sample of the polymer underwent treatment with a 1000 ppm phosphate solution (5 mL) for a duration of 6 hours. Following the mixing process, the samples were subjected to incubation under shaking conditions for a period of 6 hours. Subsequently, centrifugation and filtration procedures were employed to isolate the polymer, which had adsorbed phosphate, from the unbound phosphate ions present in the supernatant. The supernatant was then diluted to a concentration of 25 ppm, and the concentration of unbound phosphate ions was quantified using IC. The removal of adsorbed phosphate from the polymer was achieved by submerging it in a 5 mL, NaOH (0.5 N) solution with a pH of 11.5 at room temperature for a duration of 2 hours. After that, the solution was collected and analysed to quantify the recovered phosphate ions using the ion chromatography technique. Before the subsequent adsorption cycle, the pH of the polymer solution was neutralized to 7 by adding 0.1M HCl. Then, the polymer was collected via centrifugation and filtration, followed by meticulous washing with Milli-Q water to eliminate any lingering residues. The IC data reveals that the polymer has a high adsorption rate of over 78% for phosphate, and it also shows that the polymer is capable of desorbing more than 90% of the phosphate even after undergoing ten consecutive cycles.

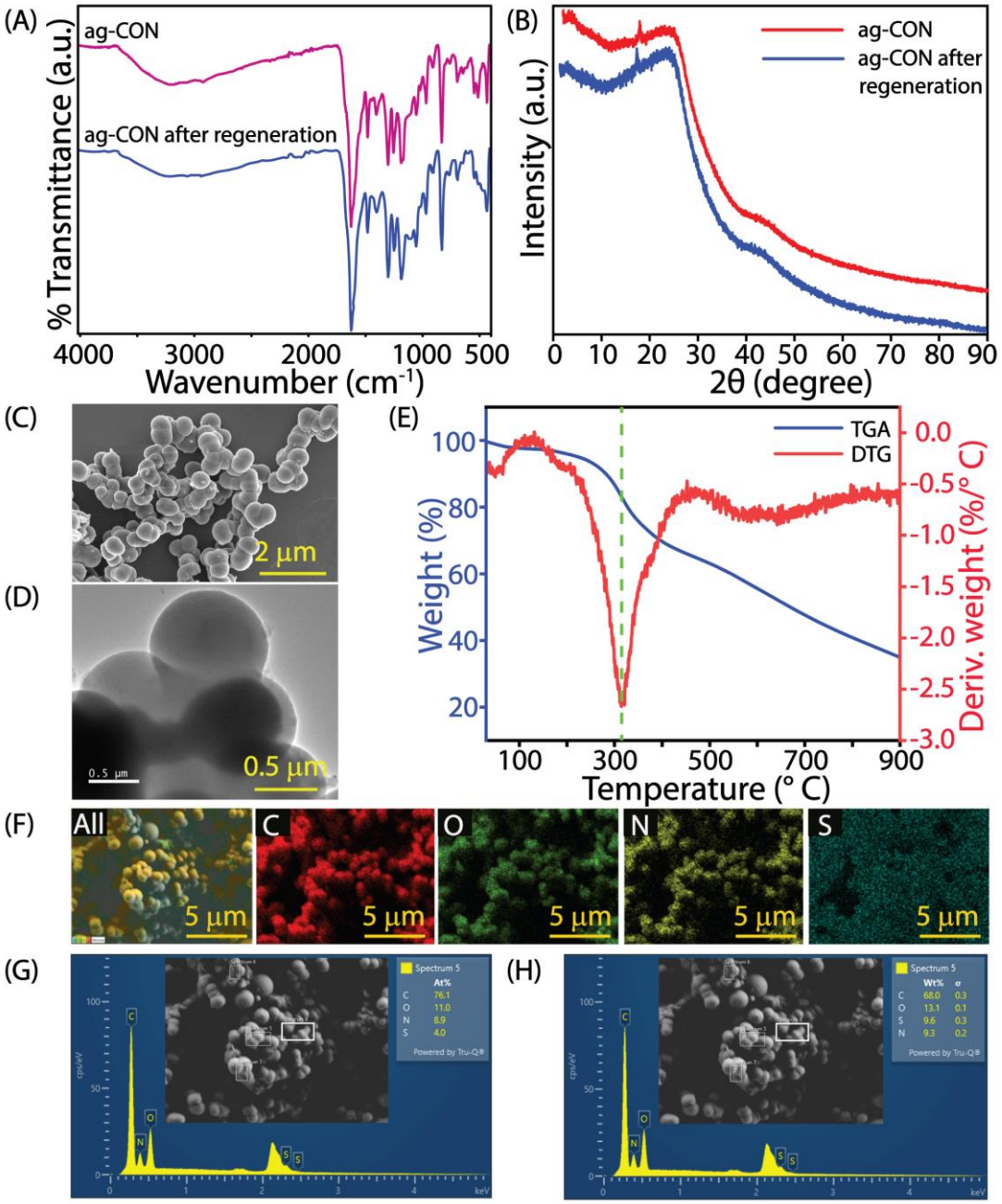

Fig. S21. FT-IR (A), PXRD (B), FESEM image (C), TEM image (D), FESEM mapping (F) and elemental analysis in atomic % (G) and weight % (H) of **ag-CON** polymer after undergoing ten cycles of regeneration.

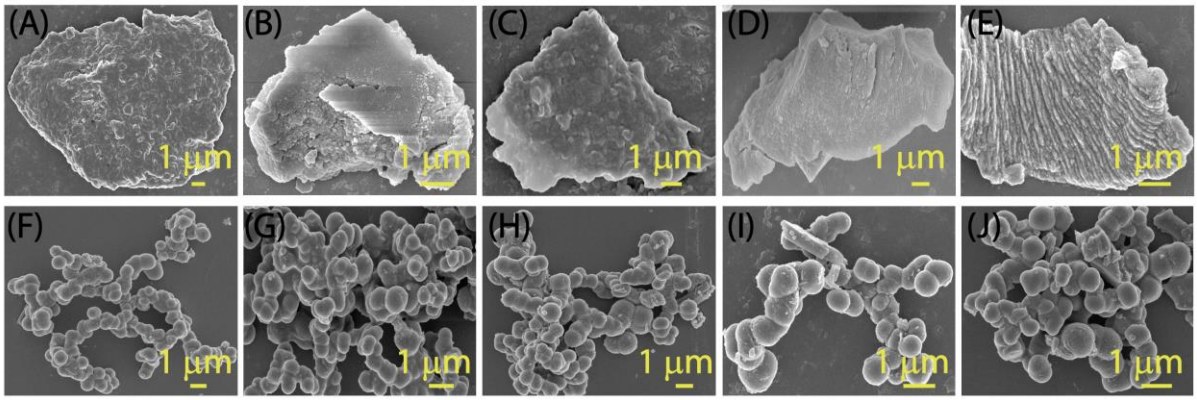

Fig. S22. FESEM images of **ag-CON** polymer after 2nd (A), 4th (B), 6th (C), 8th (D) and 10th (E) cycle of phosphate adsorption. FESEM images of **ag-CON** polymer after 2nd (F), 4th (G), 6th (H), 8th (I) and 10th (J) cycle of phosphate desorption.

5.11. Phosphate desorption kinetics — To investigate phosphate desorption kinetics from the **ag-CON** polymer, phosphate-loaded polymers (5 mg) were initially mixed with 5 mL of a 0.5 N NaOH solution (pH 11.5). The resulting solution was then subjected to continuous stirring using an orbital shaker incubator (LabTech) operating at 180 rpm and 25 °C. At varying time intervals (ranging from 50 to 1200 seconds), samples were collected, and subsequent separation of the polymers was achieved through centrifugation followed by filtration. The filtrate was subsequently diluted by a factor of 15 to maintain a phosphate concentration of 25 ppm, which was then quantified via IC. The plot t/Qt versus t (where Qt represents the amount of phosphate desorbed at time t second) exhibited conformity with the pseudo-second-order model, indicating an adsorption rate of 0.000176 mg g^{-1} min^{-1}, with a correlation coefficient (R^2) of 0.976.

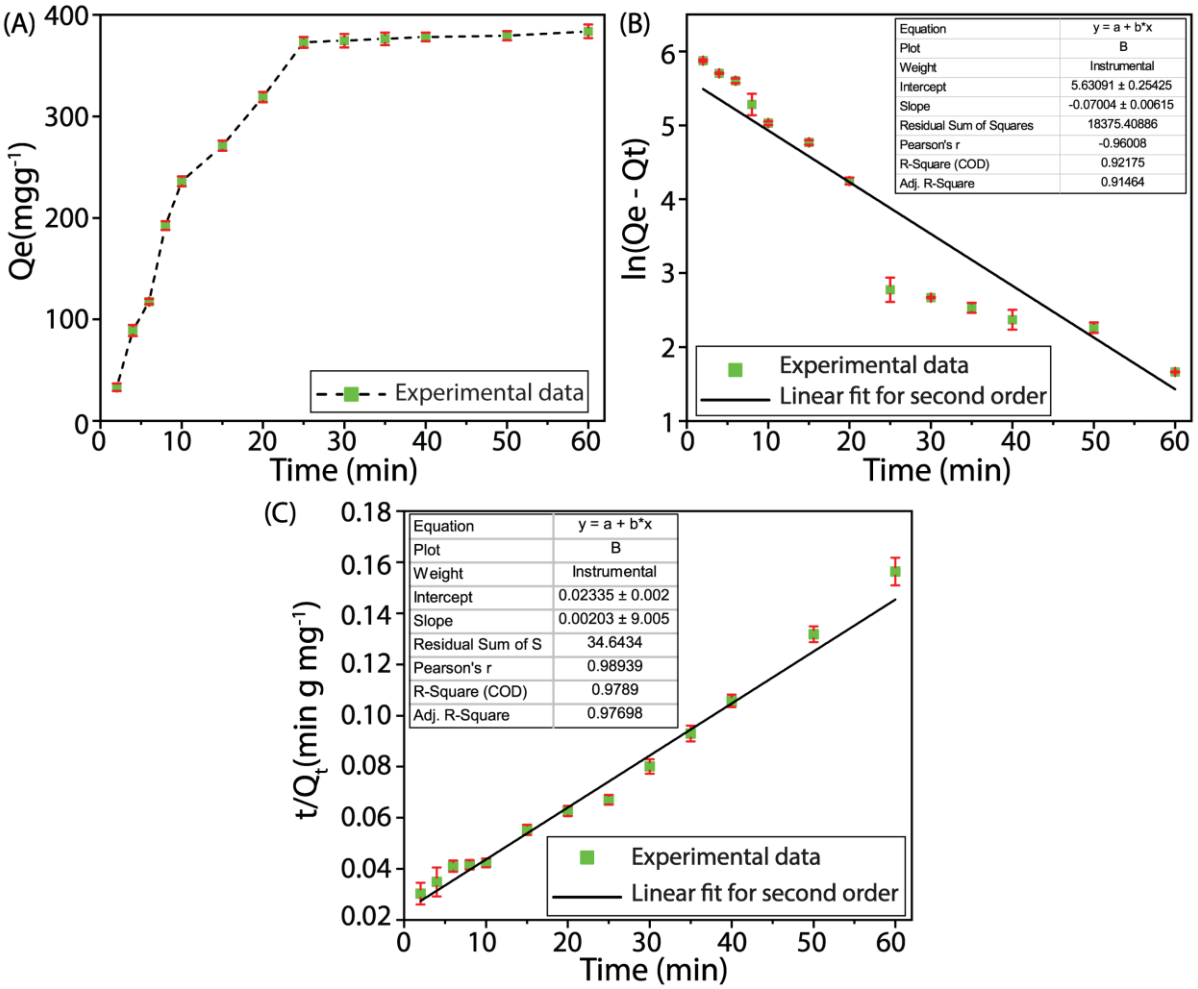

Fig. S23. Time-dependent desorption isotherm of phosphate by **ag-CON** (5mg) under room temperature(A), time-dependent desorption efficiency of **ag-CON** fitted with the first order(B) and second order kinetics(C) models.

5.12. Proposed phosphate adsorption-desorption mechanisms by the ag-CON polymer —

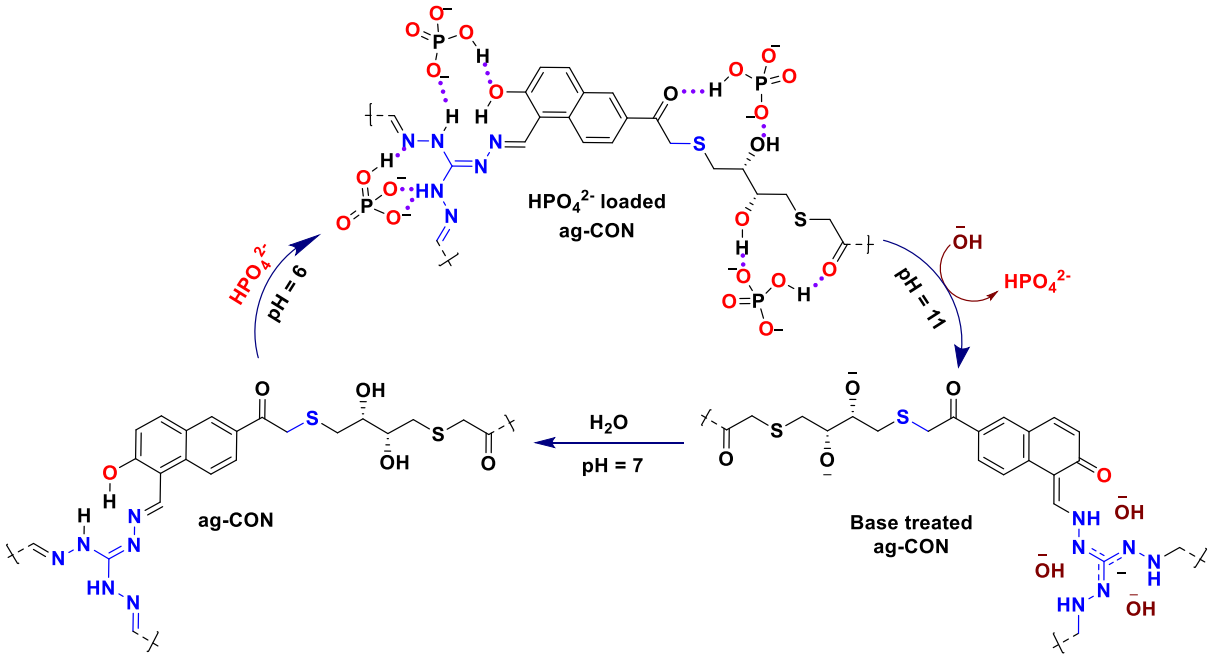

Fig. S24. Possible mechanistic pathways for adsorption and desorption process by **ag-CON** polymer.

5.13. Dynamic adsorption column experiment — An experimental setup was prepared using a glass column with a diameter of approximately 0.5 cm. The column was filled with 50 mg of the **ag-CON** polymer and 3 g of sand, creating a bed length of approximately 5 cm. Initially, 50 mL of ultrapure milli-Q water was carefully passed through the column bed to remove bubbles. After that, 500 mL of a 50 ppm aqueous phosphate solution, along with ten-fold excess other anions (F^-, Cl^-, Br^-, NO_3^-, and SO_4^{2-}), was passed through the column with a flow rate of 0.5 mL/min. The eluents from the column were collected in 10 separate 50 mL batches, and the concentration of each batch was determined using IC. Observations revealed phosphate concentrations of up to 300 mL in column eluents were lower than the level recommended by the World Health Organization (WHO). Before proceeding to the next cycle, the column was revitalized with 100 mL of a 1M NaOH solution. Experimental data revealed efficient desorption of over 93% phosphate from the polymer. The experiment was repeated for 3 cycles, consistently yielding phosphate concentrations below the WHO-recommended threshold in 250–300 mL of column eluent and efficiently removing over 90% of the phosphate from the **ag-CON** polymer after the third cycle, showcasing the ability of the polymer to effectively replicate real-time scenarios. For visual observation, two conical flasks were each filled with 10 mL of an aqueous solution comprising ammonium molybdate tetrahydrate and concentrated

nitric acid. Two columns were prepared, one containing a mixture of **ag-CON** polymer and sand in a specified ratio, while the other contained only sand. Subsequently, approximately equal volumes of 50 ppm phosphate solutions were passed through each column. A notable colour change, from colourless to yellow, was discerned in the solution of molybdate tetrahydrate and concentrated nitric acid upon elution through the sand-packed column. Conversely, no colour change was observed in the solution eluted through the column packed with **ag-CON** polymer. These visual distinctions indicate that the presence of phosphate ions in the eluent passing through the column packed with **ag-CON** polymer was significantly lower than in the sand-packed column. This leads to the conclusion that the **ag-CON** polymer efficiently adsorbed phosphate ions, resulting in minimal colour change in the solution. Conversely, in the absence of **ag-CON** polymer, the sand-packed column allowed phosphate ions to pass through, inducing the observed colour change in the solution.

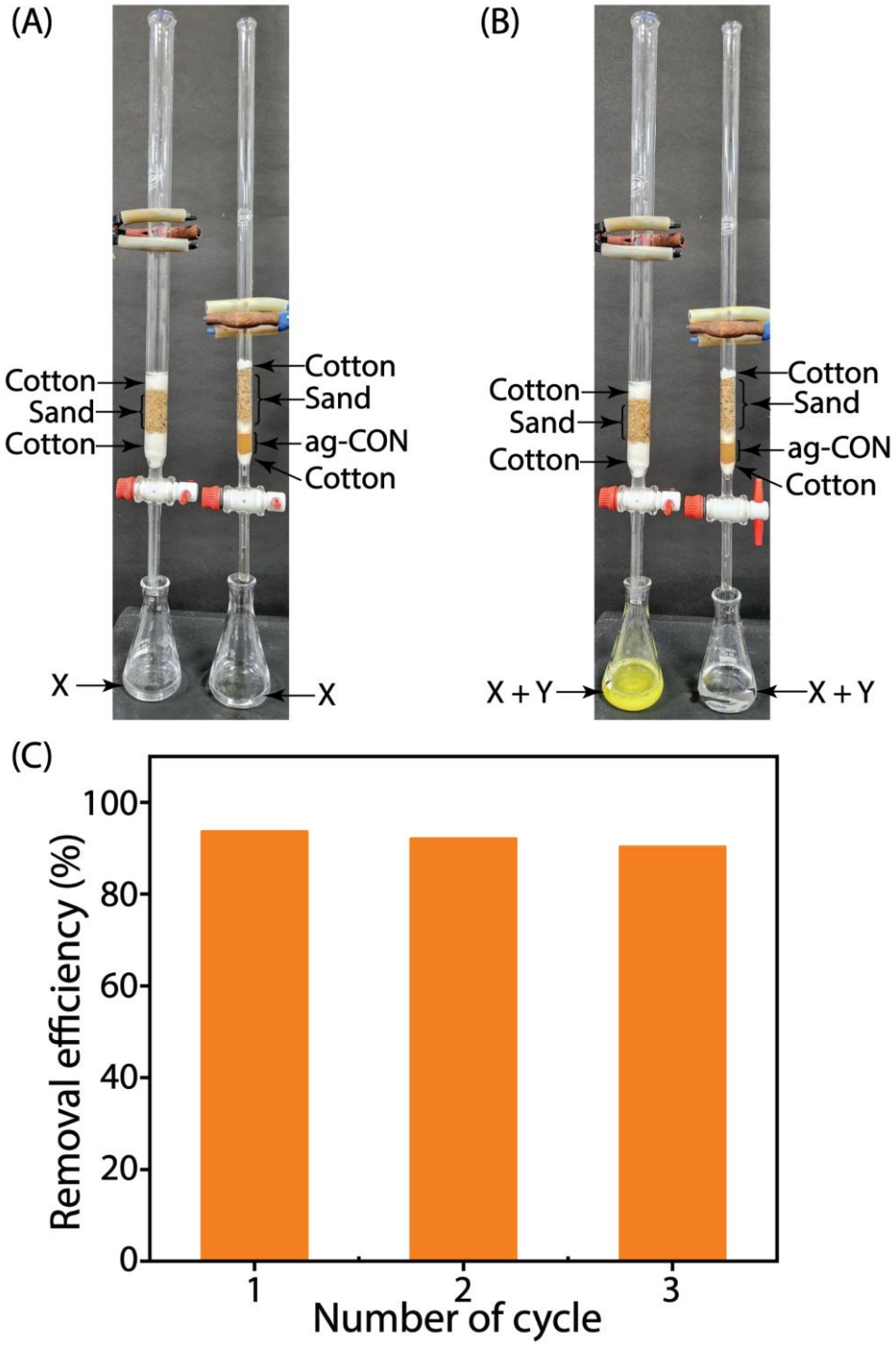

Fig. S25. Digital image for dynamic adsorption column experiment before (A) and after (B) phosphate adsorption, here X = mixture ammonium molybdate hexahydrate and concentrated HNO_3 solution, and Y = eluents that passed through the column. Phosphate ions desorption efficiency (%) of **ag-CON** polymer in adsorption column experiment (C).

Table S2. Comparison of phosphate adsorption capacity by recently reported materials.

Sl No.	Compound	Adsorption Capacity (mg/g)	pH	Equilibrium Time	Recycle	Reference
1	**ag-CON**	719	6.0	<1 min	1 N NaOH	This work
2	gCON	398	7.0	20 min	0.5 M NaOH	[3]
3	UiO-66	85	NA	2 h	0.01 M NaOH	[4]
4	UiO-66-NH_2	92	NA	2 h	0.01 M NaOH	[4]
5	UiO-66	415	7.0	5 min	Dilute HNO3	[5]
6	Zr-loaded MIL-101	20.83	6.5	6 h	0.003 M NaOH	[6]
7	Zirconium cross linked graphene oxide/alginate	255.35	NA	7h	NA	[7]
8	ZrO_2functionalized graphite oxide	16.45	6.0	436 min	0.1 M NaOH	[8]
9	Zirconium-modified zeolite	10.2	7.0	24 h	NA	[9]
10	Zr/Al-pillared montmorillonite	17.2	5.0	6 h	NA	[10]
11	ZrO2/SiO2 NM	43.8	5.0	30 min	0.1 M NaOH	[11]
12	Zr/PVA-modified PVDF membrane	21.64	7.0	30 h	NA	[12]
13	Zr-loaded orange waste gel	57	7.0	15 h	0.2 M NaOH	[13]
14	Zr-loaded wheat straw	31.9	NA	10 h	5 wt % NaOH + 5 wt % NaCl	[14]
15	ZrO_2 loaded amine crosslinked shaddock Peel	59.89	3.0	4 h	NA	[15]
16	Zr-modified activated sludge	27.55	4.0	4.5 h	NA	[16]
17	ZrO_2 loaded lignocellulosic butanol residue	7.17	6.0	250 min	NA	[17]
18	Fe3O4@SiO2@ZrO2	39.1	NA	5h	0.1 M KOH	[18]
19	Fe3O4@ZrO2	69.44	5.0	16 h	1 M NaOH	[19]
20	ZrO2@SiO2@Fe3O4	6.33	7.0	60 min	0.1 M NaOH + 1 M Na2SO4	[20]

21	ZrO2@Fe3O4	15.98	7.0	15 min	1 M NaOH	[20]
22	Zr-loaded collagen fiber	33.8	6.0	3 h	NA	[21]
23	Zirconium sulfateloaded polymer	110	7.0	2 h	NA	[22]
24	ZrO2-loaded D-201	47.9	6.5	6 h	5 % NaOH + 5 % NaCl	[23]
25	ZrO2-loaded IRA-400	91.74	NA	NA	NA	[24]
26	Zirconium molybdate-loaded anion exchange	42.2	5.5	9 h	0.1 M NaOH	[25]
27	Zr (IV)-modified chitosan	47.44	7.0	20 min	NA	[26]
28	ZrO2-loaded PANI	32.4	6.9	24 h	NA	[27]
29	Zr-loaded magnetic IPN hydrogel	50.76	6.5	20 h	0.05 M NaOH	[28]
30	MIP	78.88	NA	60 min	NA	[29]
31	ZnAl layered double hydroxide (ZnAlLDH)	57.05	NA	4 h	0.1 M NaOH	[30]
32	MCM-41	45.16	NA	10 min	NA	[31]
33	PANAF–Cl	15.49	5.0	5 min	0.3 mol L^{-1} HCl	[32]
34	CMKGM-La microspheres	16.06	4.0	10 h	0.001 M NaOH	[33]
35	MALZ	80.8	6.6	3 h	0.5 M NaOH	[34]
36	La/GTB	109 ± 4	2.5 – 7.0	30 min	0.1 NaOH	[35]
37	CTS-Fe	15.7	3.0-7.0	48 h	0.5 M NaOH	[36]
38	PMSB800	25.19	NA	24 h	NA	[37]
39	Zr/Al-pillared montmorillonite	17.2	3.0	6 h	NA	[38]
40	SA/Zr hydrogel	256.79	3.0	48 h	NA	[39]

NA = Not Available.

6. ^{1}H NMR and 13C NMR spectra of synthesized compounds —

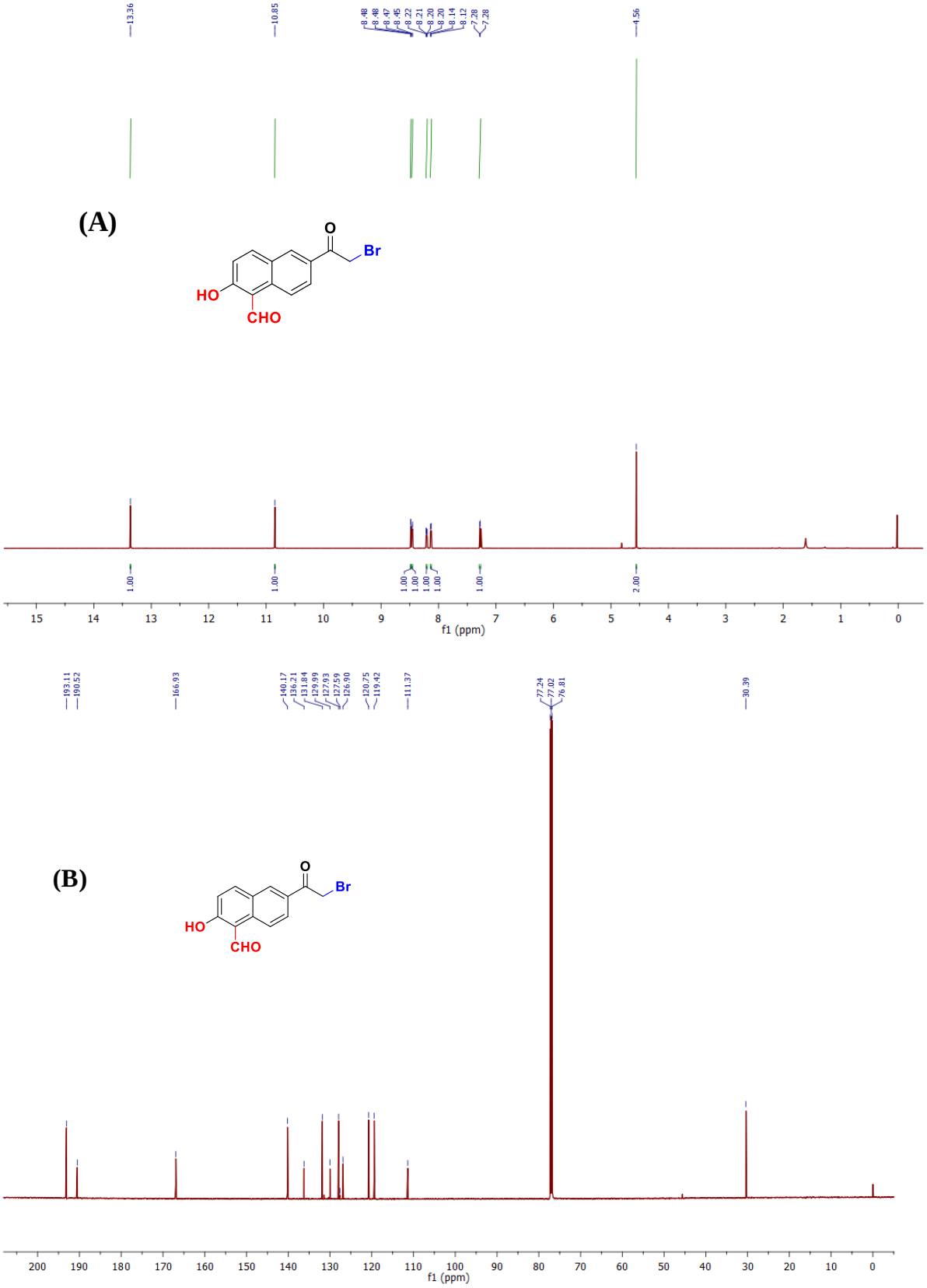

Fig. S26. ^{1}H NMR (A) and ^{13}C NMR (B) spectra of 6-(2-bromoacetyl)-2-hydroxy-1-naphthaldehyde.

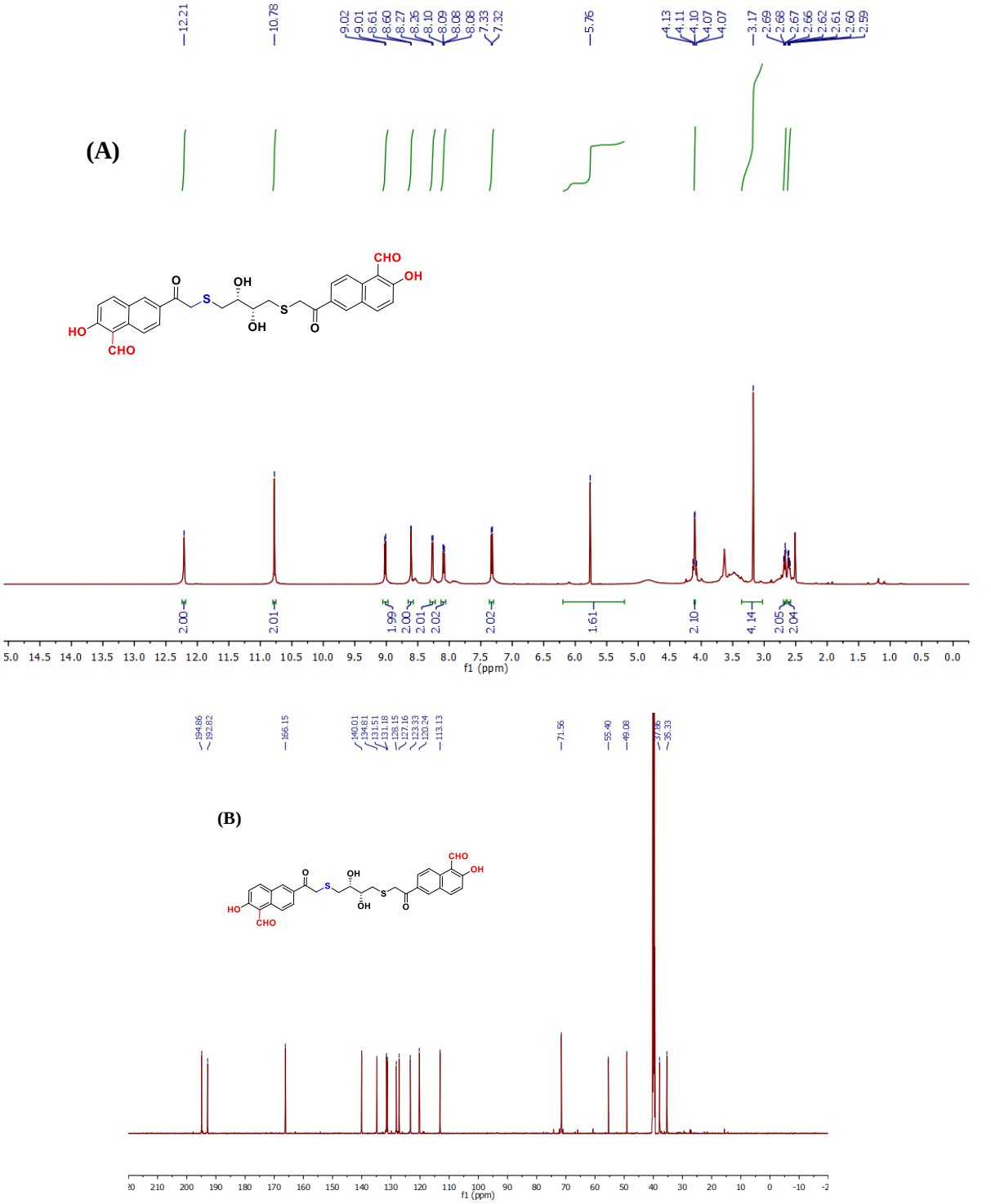

Fig. S27. ^{1}H NMR (A) and ^{13}C NMR (B) spectra of 6,6'-(2,2'-(((2R,3R)-2,3-dihydroxybutane-1,4 diyl)bis(sulfanediyl))bis(acetyl))bis(2-hydroxy-1-naphthaldehyde).

7. References —

1. B. Roy, R. Mengji, S. Roy, B. Pal, A. Jana, N. P. J. A. A. M. Singh and Interfaces, *ACS Appl. Mater. Interfaces*, 2022, **14**, 4862-4870.

2. S. D. Schnell, L. V. Hoff, A. Panchagnula, M. H. Wurzenberger, T. M. Klapötke, S. Sieber, A. Linden and K. J. C. S. Gademann, *Chem. Sci.*, 2020, **11**, 3042-3047.

3. S. Dey, S. Das, A. Patel, K. V. Raj, K. Vanka and D. J. J. o. M. C. A. Manna, *J. Mater. Chem. A*, 2022, **10**, 4585-4593.

4. K.-Y. A. Lin, S.-Y. Chen, A. P. J. M. C. Jochems and Physics, *Mater. Chem. Phys.*, 2015, **160**, 168-176.

5. Y. Gu, D. Xie, Y. Ma, W. Qin, H. Zhang, G. Wang, Y. Zhang, H. J. A. a. m. Zhao and interfaces, *ACS Appl. Mater. Interfaces*, 2017, **9**, 32151-32160.

6. T. Liu, J. Feng, Y. Wan, S. Zheng and L. J. C. Yang, *Chemosphere*, 2018, **210**, 907-916.

7. S. Shan, H. Tang, Y. Zhao, W. Wang and F. J. C. E. J. Cui, *Chem. Eng. J.*, 2019, **359**, 779-789.

8. E. Zong, D. Wei, H. Wan, S. Zheng, Z. Xu and D. J. C. E. J. Zhu, *Chem. Eng. J.* , 2013, **221**, 193-203.

9. M. Yang, J. Lin, Y. Zhan, Z. Zhu, H. J. E. S. Zhang and P. Research, *Environ. Sci. Pollut. R.*, 2015, **22**, 3606-3619.

10. W. Huang, J. Chen, F. He, J. Tang, D. Li, Y. Zhu and Y. J. A. C. S. Zhang, *Appl. Clay. Sci*, 2015, **104**, 252-260.

11. X. Wang, L. Dou, Z. Li, L. Yang, J. Yu, B. J. A. A. M. Ding and Interfaces, *ACS Appl. Mater. Interfaces*, 2016, **8**, 34668-34676.

12. D. Zhao, J. P. J. I. Chen and E. C. Research, *Ind. Eng. Chem. Res.*, 2016, **55**, 6835-6844.

13. B. K. Biswas, K. Inoue, K. N. Ghimire, H. Harada, K. Ohto and H. J. B. t. Kawakita, *Bioresource Technol.*, 2008, **99**, 8685-8690.

14. H. Qiu, C. Liang, X. Zhang, M. Chen, Y. Zhao, T. Tao, Z. Xu, G. J. A. a. m. Liu and interfaces, *Acs Appl. Mater. Inter.*, 2015, **7**, 20835-20844.

15. P. Duan, X. Xu, Y. Shang, B. Gao and F. J. J. o. t. T. I. o. C. E. Li, *J. Taiwan Inst. Chem. E*, 2017, **80**, 650-662.

16. J. Wang, X. Tong, S. J. W. Wang, Air, and S. Pollution, *Water Air Soil Pollut.*, 2018, **229**, 1-10.

17. E. Zong, X. Liu, J. Jiang, S. Fu and F. J. A. S. S. Chu, *Appl. Surf. Sci.*, 2016, **387**, 419-430.

18. A. Sarkar, S. K. Biswas and P. J. J. o. M. C. Pramanik, *J. Mater. Chem.*, 2010, **20**, 4417-4424.

19. Z. Wang, M. Xing, W. Fang and D. J. A. S. S. Wu, *Appl. Surf. Sci.*, 2016, **366**, 67-77.

20. L. Fang, B. Wu and I. M. J. C. E. J. Lo, *Chem. Eng. J.* , 2017, **319**, 258-267.

21. X.-P. Liao, Y. Ding, B. Wang, B. J. I. Shi and e. c. research, *Ind. Eng. Chem. Res.*, 2006, **45**, 3896-3901.

22. N. Pitakteeratham, A. Hafuka, H. Satoh and Y. J. W. r. Watanabe, *Water Res.*, 2013, **47**, 3583-3590.

23. L. Chen, X. Zhao, B. Pan, W. Zhang, M. Hua, L. Lv and W. J. J. o. H. M. Zhang, *J. Hazard. Mater.*, 2015, **284**, 35-42.

24. N. Y. Acelas, B. D. Martin, D. López and B. J. C. Jefferson, *Chemosphere*, 2015, **119**, 1353-1360.

25. T. H. Bui, S. P. Hong and J. J. W. r. Yoon, *Water Res.*, 2018, **134**, 22-31.

26. Q. Liu, P. Hu, J. Wang, L. Zhang and R. J. J. o. t. T. I. o. C. E. Huang, *J. Taiwan. Inst. Chem. E*, 2016, **59**, 311-319.

27. F. C. P. Masim, C.-H. Tsai, Y.-F. Lin, M.-L. Fu, M. Liu, F. Kang and Y.-F. J. E. t. Wang, *Environ. Technol*, 2019, **40**, 226-238.

28. J. Wan, C. Zhu, J. Hu, T. C. Zhang, D. Richter-Egger, X. Feng, A. Zhou and T. J. A. S. S. Tao, *Appl. Surf. Sci.*, 2017, **423**, 484-491.

29. Y. Xi, M. Huang and X. J. A. S. S. Luo, *Appl. Surf. Sci.*, 2019, **467**, 135-142.

30. Q. Yu, Y. Zheng, Y. Wang, L. Shen, H. Wang, Y. Zheng, N. He and Q. J. C. E. J. Li, *Chem. Eng. J.*, 2015, **260**, 809-817.

31. J.-W. Choi, S.-Y. Lee, S.-G. Chung, S.-W. Hong, D.-J. Kim, S.-H. J. W. Lee, Air, and S. Pollution, *Water Air Soil Poll.*, 2011, **222**, 243-254.

32. W. Zheng, Q. Wu, W. Xu, Q. Xiong, Y. K. Kalkhajeh, C. Zhang, G. Xu, W. Zhang, X. Ye, H. J. E. S. W. R. Gao and Technology, *Environ. Sci.: Water Res. Technol.*, 2022, **8**, 607-618.

33. X. Zhang, X. Lin, Y. He, Y. Chen, J. Zhou and X. J. I. j. o. b. m. Luo, *Int. J. Biol. Macromol.*, 2018, **119**, 105-115.

34. W. Shi, Y. Fu, W. Jiang, Y. Ye, J. Kang, D. Liu, Y. Ren, D. Li, C. Luo and Z. J. C. E. J. Xu, *J. Chem. Eng.*, 2019, **357**, 33-44.

35. Y. Huang, X. Lee, M. Grattieri, M. Yuan, R. Cai, F. C. Macazo and S. D. J. C. E. J. Minteer, *J.Chem. Eng.*, 2020, **380**, 122375.

36. Z. B. Zhang BoaiQi, C. N. Chen Nan, F. C. Feng ChuanPing and Z. Z. Zhang ZhenYa, *J. Chem. Eng.*, 2018.

37. M. Zhang, K. Lin, X. Li, L. Wu, J. Yu, S. Cao, D. Zhang, L. Xu, S. J. Parikh and Y. S. J. E. P. Ok, *Environ. Pollut.* , 2022, **293**, 118521.

38. J. Chen, L.-g. Yan, H.-q. Yu, S. Li, L.-l. Qin, G.-q. Liu, Y.-f. Li and B. J. C. E. J. Du, *Appl. Clay. Sci.*, 2016, **287**, 162-172.

39. Z. Qing, L. Wang, X. Liu, Z. Song, F. Qian and Y. J. C. Song, *Chemosphere*, 2022, **291**, 133103.